SAND REPORT
SAND2001-3032
Unlimited Release
Printed October 2001

Development of a Risk-Based Performance-Assessment Method for Long-Term Cover Systems—Application to the Monticello Mill Tailings Repository

Clifford K. Ho, Bill W. Arnold, John R. Cochran, Randal Y. Taira, and Stephen W. Webb

Prepared by
Sandia National Laboratories
Albuquerque, New Mexico 87185 and Livermore, California 94550

Sandia is a multiprogram laboratory operated by Sandia Corporation, a Lockheed Martin Company, for the United States Department of Energy under Contract DE-AC04-94AL85000.

Issued by Sandia National Laboratories, operated for the United States Department of Energy by Sandia Corporation.

Available to DOE and DOE contractors from
U.S. Department of Energy
Office of Scientific and Technical Information
P.O. Box 62
Oak Ridge, TN 37831

Telephone: (865)576-8401
Facsimile: (865)576-5728
E-Mail: reports@adonis.osti.gov
Online ordering: http://www.doe.gov/bridge

Available to the public from
U.S. Department of Commerce
National Technical Information Service
5285 Port Royal Rd
Springfield, VA 22161

Telephone: (800)553-6847
Facsimile: (703)605-6900
E-Mail: orders@ntis.fedworld.gov
Online order: http://www.ntis.gov/ordering.htm

SAND2001-3032
Unlimited Release
Printed October 2001

Development of a Risk-Based Performance-Assessment Method for Long-Term Cover Systems—Application to the Monticello Mill Tailings Repository

Clifford K. Ho, Bill W. Arnold, John R. Cochran, and Stephen W. Webb
Sandia National Laboratories
P.O. Box 5800
Albuquerque, New Mexico 87185
Contact: ckho@sandia.gov
(505) 844-2384

Randal Y. Taira
Pacific Northwest National Laboratory
4500 Sand Point Way NE, Suite 100
Seattle, WA 98105

Abstract

A probabilistic, risk-based performance-assessment methodology is being developed to assist designers, regulators, and involved stakeholders in the selection, design, and monitoring of long-term covers for contaminated subsurface sites. This report presents an example of the risk-based performance-assessment method using a repository site in Monticello, Utah. At the Monticello site, a long-term cover system is being used to isolate long-lived uranium mill tailings from the biosphere. Computer models were developed to simulate relevant features, events, and processes that include water flux through the cover, source-term release, vadose-zone transport, saturated-zone transport, gas transport, and exposure pathways. The component models were then integrated into a total-system performance-assessment model, and uncertainty distributions of important input parameters were constructed and sampled in a stochastic Monte Carlo analysis. Multiple realizations were simulated using the integrated model to produce cumulative distribution functions of the performance metrics, which were used to assess cover performance for both present- and long-term future conditions. Performance metrics for this study included the water percolation reaching the uranium mill tailings, radon flux at the surface, groundwater concentrations, and dose. Results of this study can be used to identify engineering and environmental parameters (e.g., liner properties, long-term precipitation, distribution coefficients) that require additional data to reduce uncertainty in the calculations and improve confidence in the model predictions. These results can also be used to evaluate alternative engineering designs and to identify parameters most important to long-term performance.

Acknowledgments

This work was funded by the U.S. Department of Energy EM-50 Technical Task Plan AL21SS22 “Risk-Based Performance Assessment of Long-Term Cover Designs for Waste Isolation and Disposal at DOE Facilities.” Sandia is a multiprogram laboratory operated by Sandia Corporation, a Lockheed Martin Company, for the United States Department of Energy under Contract DE-AC04-94AL85000.

Contents

1. Introduction 9

2. Description of Performance-Assessment Process 10

3. Description of Monticello Mill Tailings Repository Site 12

3.1 Background 13

3.2 Regulatory Requirements and Performance Metrics 15

3.2.1 Regulatory History 15

3.2.2 Records of Decision 15

3.2.3 Identification of Landfill-Design Regulations 16

3.2.4 Summary of Performance Metrics for the Monticello Repository 19

4. Performance Assessment of the Monticello Mill Tailings Repository 21

4.1 Scenario Development and Screening of FEPs 21

4.2 Total-System Framework Model 26

4.3 Process-Model Development and Parameter Distributions 28

4.3.1 Water Percolation through the Cover 28

4.3.2 Radon Gas Transport through the Cover 32

4.3.3 Source-Term Release 36

4.3.4 Vadose-Zone Transport 38

4.3.5 Saturated-Zone Transport 40

4.3.6 Human Exposure 42

4.4 Results and Discussion 44

4.4.1 Percolation through the Cover 44

4.4.2 Radon Gas Flux at the Surface 46

4.4.3 Groundwater Concentration and Exposure Assessment for the Shallow Alluvial Aquifer 48

4.4.4 Groundwater Concentration and Exposure Assessment for the Burro Canyon Aquifer 51

5. Summary and Conclusions 52

6. References 54

Appendix A: Parameter Values and Distributions for Material Properties of the Monticello Cover 59

Uncertainty Distributions for Layer 1 60

Uncertainty Distributions for Layers 2 and 4 62

List of Figures

Figure 1. Integration between performance-assessment task and other primary tasks in the long-term capping strategy. 12

Figure 2. Map of the Monticello Mill Tailings site and vicinity. 13

Figure 3. Aerial view of the double composite-liner system at the base of the repository. 14

Figure 4. Illustration of the landfill cover and geology. 14

Figure 5. Conceptual model for percolation (scenarios 1 and 2) and gas transport (scenarios 3 and 4) through the cover for present and future conditions. A 3% slope is assumed for the drainage layer. 24

Figure 6. Conceptual model for radionuclide transport from the mill tailings to the shallow alluvial aquifer and location of receptor well for present (scenario 5) and future (scenario 6) conditions. 25

Figure 7. Conceptual model for radionuclide transport from the mill tailings to the deep Burro Canyon aquifer and location of receptor well for present (scenario 7) and future (scenario 8) conditions. 25

Figure 8. Screen capture of FRAMES graphical user interface for scenario 5. 27

Figure 9. Cumulative probability distribution of water percolation reaching the mill tailings for present and future conditions (scenarios 1 and 2). 45

Figure 10. Cumulative probability distribution of water percolation reaching the mill tailings for present and future conditions for an alternative ET cover design. 46

Figure 11. Cumulative probability distribution of simulated radon flux at the land surface for present and future conditions (scenarios 3 and 4). 47

Figure 12. Cumulative probability distribution for peak Ra-226 concentration in the shallow alluvial aquifer for present and future conditions (scenarios 5-6). Note: concentration values of 0 are not plotted on the log scale. 49

Figure 13. Cumulative probability distribution for peak cumulative dose for Ra-226 and its progeny from the shallow alluvial aquifer for present and future conditions (scenarios 5-6). Note: dose values of 0 are not plotted on the log scale. 50

Figure 14. Cumulative probability distribution for peak cumulative dose for Ra-226 and its progeny from the Burro Canyon aquifer for future conditions (scenario 8). Note: dose values of 0 are not plotted on the log scale. 52

List of Tables

Table 1. Summary of performance objectives applicable to the Monticello Mill Tailings Repository. 20

Table 2. List of features, events, and processes relevant to the Monticello Mill Tailings Repository. 21

Table 3. Summary of scenarios and performance objectives evaluated in this study. 22

Table 4. Uncertainty distributions for stochastic parameters in the percolation model. 30

Table 5. Correlation coefficients between parameters in the percolation model. 32

Table 6. Parameter values for radon flux model (present conditions). 33

Table 7. Parameter values for radon flux model (future conditions). 34

Table 8. Parameter values for source-term model. 37

Table 9. Parameter values for double composite-liner system in vadose-zone model. 39

Table 10. Parameter values for vadose-zone layer for two aquifers. 40

Table 11. Parameter values for saturated-zone model. 41

Table 12. Parameter values for chronic exposure module. 43

Table 13. Parameter values for receptor intake module. 43

Table 14. Parameter values for human health impact module. 43

Table 15. Summary of parameters important to simulated water percolation through the cover based on stepwise linear-regression analysis. 44

Intentionally Left Blank

1. Introduction

Long-term cover systems are needed at U.S. Department of Energy (DOE) complexes to assist in isolating contaminants and waste that have migrated into the subsurface near landfills, waste-disposal sites, and high-level waste tanks. The long-term covers are considered to be a vital remedial option for DOE's 2006 Accelerated Cleanup Plan (DOE/EM-0362), which intends to clean up more than 90 percent of the contaminated sites in DOE's Environmental Management Program. In addition, DOE Order 435.1 states that performance assessments are to be conducted for low-level waste disposed after September 26, 1988, and that performance objectives should be evaluated for a 1,000-year period to determine potential risk impacts to the public and environment. However, current landfill-cover design guidelines, such as those stated in the Resource Conservation and Recovery Act, are not risk-based and do not consider long-term site-specific influences such as climate, vegetation, and soils. These design guidelines may not address important long-term features, events, and processes at the site that may contribute to the long-term risk of groundwater contamination and human exposure. In addition, traditional design guidelines for covers often rely on deterministic models of flow and transport processes that neglect uncertainty inherent in actual contaminant transport.

As a result, a probabilistic, risk-based performance-assessment methodology is being developed to assist designers, regulators, and involved stakeholders in the selection, design, and monitoring of long-term covers. This approach considers regulatory requirements, site-specific parameters, engineering-design parameters, and long-term verification and monitoring requirements. Because many of the contaminants are long-lived, this methodology also considers changes in the environmental setting (e.g., precipitation, temperature) and cover components (e.g., liner integrity) for long time periods (>100 years). Uncertainty and variability in important site-specific parameters are also incorporated through stochastic simulations in this method.

Additional benefits of a risk-based performance-assessment method include potential savings in cost, increased public confidence, and useful guidance for associated studies in engineering design, environmental setting, and long-term monitoring. The design and implementation of long-term covers can be very costly, especially if prototypes are designed and implemented without meaningful criteria, leading to poor performance that may violate exposure limits set by regulatory requirements. The inclusion of uncertainty distributions for important input parameters (e.g., material properties, precipitation) addresses the performance of long-term covers under more realistic (and uncertain) conditions and ensures more defensible calculations of long-term performance.

Using performance metrics such as water percolation through the waste, groundwater concentrations, and dose also provides a more concrete metric against which alternative designs can be compared for performance and cost. In addition, the integrated approach of the performance-assessment model ensures a comprehensive, defensible, and traceable process that demonstrates the design selection process in a systematic fashion to regulators and stakeholders, reducing the likelihood of providing costly re-evaluations and demonstrations to address features, events, or processes that were not considered initially. Finally, the results of the performance assessment can be used by associated studies in engineering design, environmental setting, and long-term performance to identify parameters that are most important to long-term

performance. These parameters may require additional characterization and monitoring by these groups to reduce the uncertainty in the calculations and to improve the confidence in the models.

The overall objective of this study is to provide these methods and tools to DOE and to document the results in a guidance document that will be available to end-users to implement long-term cover systems. The guidance will describe the demonstrated methodology along with recommended processes and models that are appropriate to various sites. An "if-then" flow chart will be developed to assist the end-user in deciding on the appropriate tools, methods, and models to use in their performance assessment. For example, sites can be initially grouped according to current environmental settings (e.g., arid, semi-arid, sub-humid, and humid). For each environmental setting, FEPs (features, events, and processes) that have been found to be important for these conditions will be listed, along with viable cover designs. Recommended models and software tools that will be readily available for the end-user will also be identified and described. Examples for various performance assessments using different environmental conditions and cover designs will also be provided and discussed.

In this paper, we first define a performance assessment and describe the systematic process to conduct a performance assessment for long-term covers. This method is then illustrated using the Monticello Mill Tailings Repository Site in Monticello, Utah. A general description of the site is provided, and four primary performance objectives based on regulatory requirements are presented. A performance assessment of the repository at the Monticello Mill Tailings Site is then detailed, starting with a description of the conceptual site model and scenarios to be considered. A framework tool for conducting a stochastic analysis is briefly described, followed by a detailed description of each feature, event, and process that is modeled and integrated into the framework tool. Results of the model are then presented and compared to the performance metrics. Conclusions are drawn regarding the performance of the existing cover at Monticello, and comments and recommendations regarding the proposed performance-assessment method for long-term covers are presented.

2. Description of Performance-Assessment Process

As defined by DOE M 435.1-1, a performance assessment is "An analysis of a radioactive waste disposal facility conducted to demonstrate there is a reasonable expectation that performance objectives established for the long-term protection of the public and the environment will not be exceeded following closure of the facility." In addition, DOE M 435.1-1 also states that the method used for the performance assessment must include uncertainty analyses. A method that addresses these requirements has been used for the Waste Isolation Pilot Plant (DOE, 1996) and Yucca Mountain Project (DOE, 1998) to assess the long-term performance of nuclear waste repositories. Uncertainty analyses and probabilistic approaches have also been used for decommissioning of contaminated sites (Meyer and Gee, 1999; Meyer and Taira, 2001). A similar systematic approach is proposed here to conduct performance assessments for long-term covers. The approach is outlined as follows:

1. Develop and screen scenarios based on regulatory requirements (performance objectives) and relevant features, events, and processes

2. Develop models of relevant features, events, and processes

3. Develop values and/or uncertainty distributions for input parameters

4. Perform calculations and sensitivity/uncertainty analyses

5. Document results and provide feedback to previous steps and associated areas to improve calculations, as needed

In step 1, a scenario is identified as a well-defined sequence of features, events and processes that describes possible future conditions at the disposal site. An example of a scenario is the release of radionuclides from a landfill via the vadose zone to the aquifer, where water is pumped from a well and ingested by an individual. Another scenario might be the inadvertent intrusion of a person digging for natural resources, which disrupts the repository and causes a direct release of radionuclides to the surface. The decision to evaluate or not evaluate various scenarios depends, in part, on relevant performance objectives set forth by regulatory requirements. In addition, scenarios should be chosen that represent features, events, and processes that are relevant to the specific site being evaluated. More information regarding features, events, and processes that are modeled in this study is provided in Section 4.1.

Step 2 develops the models that are necessary to simulate the chosen scenarios in the performance assessment. The models that are used vary in complexity, and a hierarchy of models can exist. An overarching conceptual model of each scenario is developed to guide the development of more detailed mechanistic models of individual features, events, and processes that comprise the scenario. These detailed models are then integrated into a total-system model of the entire scenario. The integration of the more detailed models may include the models themselves or a simplified abstraction of the model results. An example of this model development is provided in Sections 4.2 and 4.3.

After the models are developed, values must be assigned to the parameters required by the model (step 3). If the parameter is well characterized, a single deterministic value may be assigned. However, uncertainty and/or variability in the parameter may require the use of distributions (e.g., log-normal, uniform, etc.) to define the values. Experimental data, literature sources, and professional judgment are often used to determine these distributions. The development of uncertainty distributions for parameters used in this study are described in Section 4.3.

In step 4, calculations are performed using the integrated total-system model. Because stochastic parameters are used, a Monte Carlo approach is taken to create an ensemble of simulations that use different combinations of the input parameters. For each run (realization), a value for each input parameter is sampled from the uncertainty distribution, and the simulation is performed. The results of each realization are equally probable, and the collection of simulation results yields an uncertainty distribution that can be compared to performance objectives to assess the risk of exceeding those performance objectives or metrics. Sensitivity analyses can also be performed to determine which parameters the performance metrics are most sensitive to.

The last step (step 5) is to document the findings, typically as cumulative distribution functions that present the probability (or risk) of exceeding a performance objective. These findings may

be used to evaluate alternative designs, where performance objectives, cost, and schedule comprise some of the criteria in choosing the most suitable cover for a site.

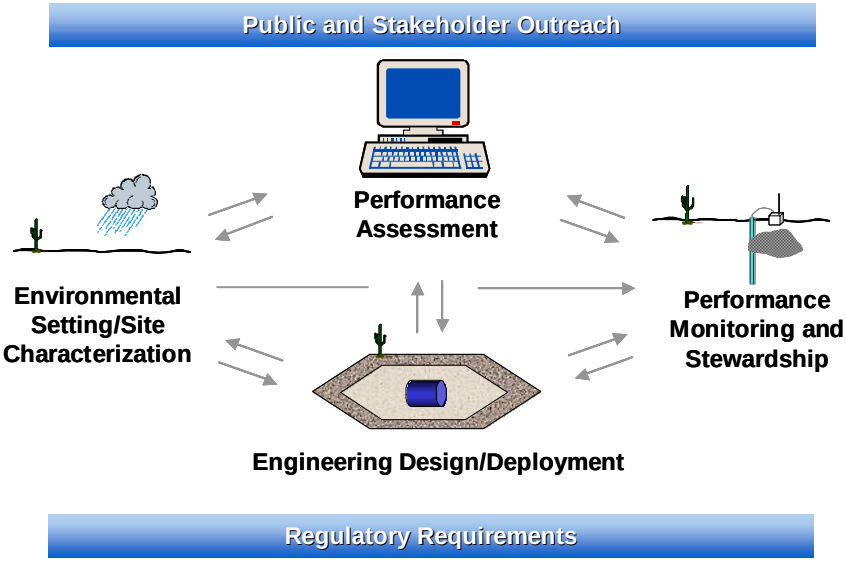

Figure 1. Integration between performance-assessment task and other primary tasks in the long-term capping strategy.

Finally, within this long-term capping strategy, an integrated effort must occur among several major components to accomplish a performance assessment (see Figure 1). The performance assessment relies on information from the Environmental Setting Task (e.g., climate change, vegetation change, etc.) and Engineering Design Task (e.g., material properties, configuration, etc.). In return, results from the performance assessment will identify parameters that are most important to long-term performance. More data can then be obtained on these parameters to reduce uncertainty. In addition, the parameters that are most important to performance can be used by the Long-Term Monitoring Task to assess methods to monitor these parameters important to long-term performance. Therefore, a performance assessment can be an iterative process, where each iteration builds upon previous information to continually improve the confidence in the calculations.

3. Description of Monticello Mill Tailings Repository Site

To illustrate the application of the performance-assessment method for long-term covers, an example is provided using the uranium mill tailings repository at the Monticello Mill Tailings Site in Monticello, Utah. A brief overview of the site is provided in this section, along with the performance objectives for this site. The performance-assessment method for this site is then detailed in Section 4.

3.1 Background

The Monticello Mill Tailings Site is located in southeastern Utah, south of the town of Monticello (see Figure 2). The present climate at Monticello is "sub-humid," with an average annual precipitation of ~38 cm (15 inches) and an average annual temperature of 7.8 ºC (46 ºF).

In 1941, the Monticello mill was constructed and used to process nearly a billion kilograms of ore. By 1960, when operations were terminated, approximately 2 million cubic meters of low-level radioactive uranium mill tailings had been left behind from the operations. These mill tailings are sand-like material that remains after uranium has been extracted from the ore, and the tailings contain radioactive materials that can produce radon gas and gamma radiation.

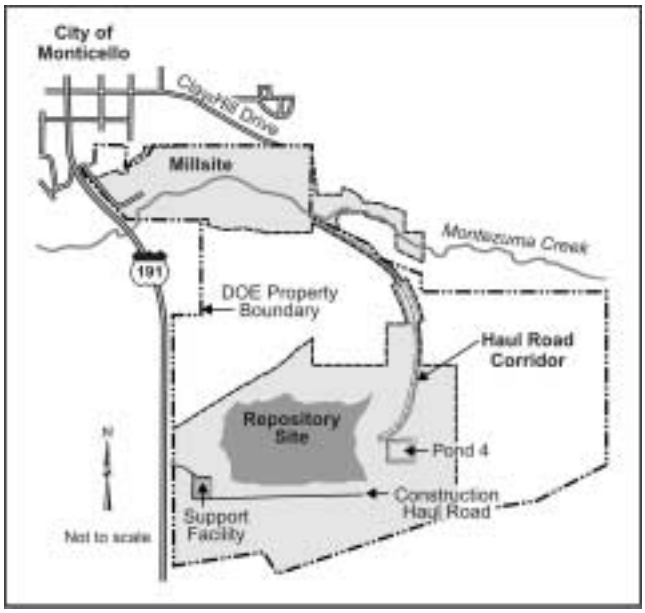

Figure 2. Map of the Monticello Mill Tailings site and vicinity.

To contain the mill tailings, DOE began construction of a repository south of the original mill site in 1995, and in 1996 the construction of a composite double-liner system at the base of the repository was completed (see Figure 3). Trucks were used to transport the tailings from the mill site to the repository beginning in 1997, and placement of the tailings was completed in 1999. Construction of the cover began during the placement of the tailings, and, although the majority of the cover is complete, re-vegetation of the entire cover is being finalized. The cover was designed to mitigate the release of radon gas to the surface and to minimize water infiltration to the mill tailings. It consists of a thick topsoil layer with vegetation that can store precipitation and allow evaporation and transpiration via the vegetation. This top layer overlies a coarse sand layer that acts as a capillary barrier and is intended to drain any infiltrating water laterally above a high-density polyethylene geomembrane. Beneath the geomembrane is a compacted clay layer that serves as a barrier to radon gas transport and water infiltration. The clay layer rests directly

on top of the mill tailings. At the base of the repository beneath the mill tailings is a double composite-liner system composed of sand, two geomembrane liners, two geosynthetic clay-liners, and a transmissive leachate collection system. The entire repository is surrounded by Quaternary deposits consisting of sandy loam, clay, and pediment gravels.

Figure 3. Aerial view of the double composite-liner system at the base of the repository.

Beneath the repository, two groundwater-bearing units (aquifers) exist. The upper unit is called the alluvial aquifer, which is a perched aquifer located as close as several meters below the bottom of the repository. This alluvial aquifer discharges to Montezuma Creek in several areas east of the millsite, and it had been contaminated by mill tailings prior to construction of the repository. The contaminants of concern include uranium, as well as its radioactive decay products (thorium-230, radium-226, radon-222), and heavy metals such as vanadium, lead-210, and arsenic. The lower regional aquifer beneath the alluvial aquifer is called the Burro Canyon aquifer and has not been contaminated. Between the alluvial aquifer and the Burro Canyon aquifer are unsaturated layers of shale and sandstone. The water from the upper alluvial aquifer is used for irrigation purposes, but all drinking-water wells are located in the lower Burro Canyon aquifer. An illustration of the repository site and the geologic formations beneath it are shown in Figure 4.

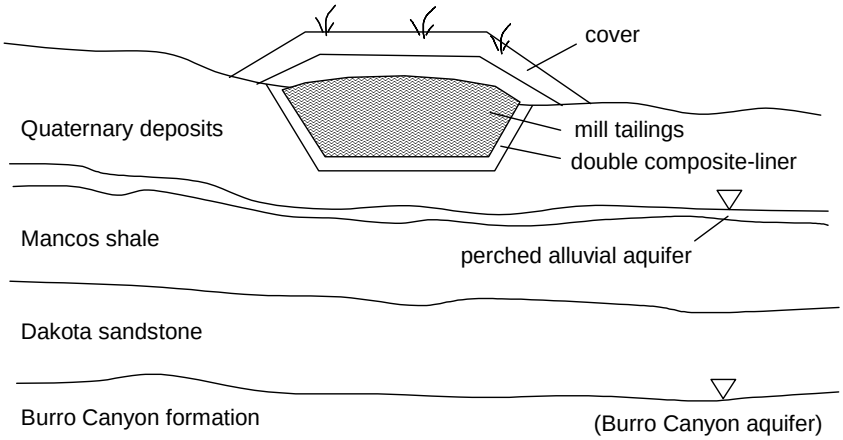

Figure 4. Illustration of the landfill cover and geology.

3.2 Regulatory Requirements and Performance Metrics

Waste-disposal sites are designed to be protective of human health and the environment. The phrase "protective of human health and the environment" expresses a clear intent, but the phrase does not have a universally accepted meaning. For example, should protective measures be designed to be effective for a few generations (~ 100 years) or so long as the waste could present a hazard? For illustrative purposes, this section identifies the quantitative performance objectives set by regulations applicable to the landfill being built as part of the closure of the Monticello Mill Tailing Site. Insight for this regulatory analysis was provided by DOE (1995) and MACTEC (2000).

Long-lived contaminants will remain at many of the DOE closure sites, including the Monticello landfill. To address the long-term management of these closure sites, the DOE has created a "stewardship" program, which is discussed after the identification of the quantitative performance objectives.

3.2.1 Regulatory History

Congress found that active and inactive uranium- and thorium-mill operations might pose a potential and significant health hazard to the public, and in 1978 Congress passed the Uranium Mill Tailings Radiation Control Act (UMTRCA) to assess and remediate hazards at 24 privately owned mill sites. Title I of UMTRCA authorizes the DOE to clean up these 24 sites to meet 40 CFR 192 standards set by the U.S. Environmental Protection Agency (EPA), with the concurrence of the U.S. Nuclear Regulatory Commission.

UMTRCA did not address the Monticello Mill Tailings Site because the site is not privately owned; the DOE owns the site. In 1980 the DOE accepted the Monticello Mill Tailings Site under DOE's Surplus Facilities Management Program. In 1988, the DOE, EPA, and the State of Utah entered into a Federal Facilities Agreement. EPA included the site on the Comprehensive Environmental Response, Compensation and Liability Act (CERCLA) National Priorities List (NPL) in 1989. Studies undertaken in 1989 identified on-site and off-site contamination of groundwater and stream sediments. Contaminates of concern include arsenic, chromium, lead, molybdenum, selenium, and vanadium, and the radioactive materials included radium-226, radon, and uranium.

Three operable units were defined. Operable Unit 1 addresses the mill tailings and other contaminated materials at the old millsite. Operable Unit 2 addresses remediation of other, peripheral properties that were contaminated by radioactive materials from the millsite. Operable Unit 3 addresses contaminated groundwater and surface water down gradient of the millsite.

3.2.2 Records of Decision

Remedial actions were selected through two Records of Decisions (RODs). To address threats to human health from Operable Units 1 and 2, the first ROD was issued in 1990. (EPA/ROD/R08-90/034). The second ROD was issued in 1998 and addressed threats posed by Operable Unit 3.

The first ROD requires consolidation of contaminated materials from the millsite and the peripheral properties in a new repository that is being built ~2 km south of the old millsite. The ROD requires:

- Removal of tailings, ore, and process-related material from their Millsite location
- De-watering contaminated materials to bring moisture content to 0.26 or less
- Placement of the contaminated materials in a landfill that is being constructed ~2 km south of the millsite
- Design of the landfill to meet requirements of the UMTRCA and 40 CFR 192 technical standards. To meet these requirements, the landfill will be:
  - Capped to protect the groundwater, to isolate the waste from the environment, and to control the escape of radon gas
  - Constructed with features to control and treat surface-water runoff
  - Revegetated
- Long-term surveillance and environmental monitoring will be implemented to ensure the effectiveness of the remedial action and compliance with groundwater and surface-water standards
- Approximately two million cubic meters of contaminated materials will be consolidated in the ~32 square kilometer (80 acre) landfill

In addition, there are numerous federal regulations, state regulations, and guidance documents that can be applied to the design of the landfill that receives the mill tailings and associated wastes. The next section discusses the identification of those regulations.

3.2.3 Identification of Landfill-Design Regulations

As required by CERCLA, the protection levels achieved by the landfill system must be at least equal to those specified by *applicable or relevant and appropriate requirements* (ARARs). The primary ARARs for the new landfill are:

(A) EPA's 40 CFR 192, "Health and Environmental Protection Standards for Uranium and Thorium Mill Tailings;" these are the Federal regulations implementing UMTRCA

(B) EPA's 40 CFR 141 and 40 CFR 143, "Safe Drinking Water Act National Primary and Secondary Drinking Water Standards"

(C) "Administrative Rules for Ground Water Quality Protection" (UAC R3l7-6), the State regulations implementing parts of the Utah Water Quality Act (Title 19, Chapter 5, Utah Code Annotated)

(D) "Standards for Owners and Operators of Hazardous Waste Treatment, Storage, and Disposal Facilities" (R315-8, Utah Administrative Code), the State regulations implementing parts of the Utah Solid and Hazardous Waste Act (Title 19, Chapter 6, Part 1, Utah Code Annotated)

(E) DOE Order 435.1, Radioactive Waste Management

Each of these primary ARARs is discussed below.

(A) Landfill Requirements from the EPA's 40 CFR 192

The EPA's 40 CFR 192 sets two specific standards for radon releases from landfills containing mill tailings. It states that the control of residual radioactive materials and their listed constituents shall be designed to:

(1) Be effective for up to one thousand years, to the extent reasonably achievable, and, in any case, for at least 200 years

(2) Provide reasonable assurance that releases of radon-222 from residual radioactive material to the atmosphere will not:

(i) Exceed an average release rate of 20 picocuries per square meter per second

(ii) Increase the annual average concentration of radon-222 in air at or above any location outside the disposal site by more than one-half picocurie per liter (40 CFR 192.02)

40 CFR 192.02 also sets groundwater protection standards for uranium mill tailings that are similar to RCRA regulations concerning hazardous waste. The mill tailings standards include Maximum Contaminant Levels (MCLs) for a number of contaminants, including arsenic, lead, radium, uranium, and gross alpha-particle activity (excluding radon and uranium). Under 40 CFR 192, the point of compliance (POC) for groundwater protection is the intersection of a vertical plane with the uppermost aquifer underlying the site, located at the hydraulically downgradient limit of the disposal area plus the area taken up by any liner, dike, or other barrier designed to contain the residual radioactive material (40 CFR 192.02(c)(4)).

(B) Federal Safe Drinking Water Act

The EPA's 40 CFR 141 and 40 CFR 143 set health-based standards (maximum contaminant levels or MCLs) for community water-supply systems. For contaminants present at the Mill Tailings Site, the Safe Drinking Water Act MCLs are all equal to, or higher than, the groundwater protection standards set in 40 CFR 192.

For example, the Safe Drinking Water Act (SDWA) MCL for selenium is 0.05 milligrams per liter (mg/L), and the groundwater protection standard set in 40 CFR 192 is 0.01 mg/L; therefore, use of the 40 CFR 192 standards provides equal or greater protection than that provided by the SDWA. The only exception is that the SDWA sets an MCL of 4 millirem per year (mrem/yr) for

beta particles and photon radiation from man-made radionuclides, and 40 CFR 192 has no standard for beta particles.

(C) Landfill Requirements from the Utah Water Quality Act

The administrative Rules for Ground Water Quality Protection (UAC R317-6) implement a State environmental law that has no Federal counterpart. Because many of its provisions are more stringent than those in other ARARs, UAC R317-6 governs most aspects of groundwater protection. UAC R317-6 applies to all groundwater in the State and defines groundwater as "subsurface water in the zone of saturation including perched groundwater."

This extends the protectiveness of the rule beyond that of the RCRA and UMTRCA regulations, which apply only to aquifers that can yield significant quantities of water to wells or springs. The Utah definition of contaminant is not restricted to hazardous substances. Instead, a contaminant is "any physical, chemical, biological, or radiological substance or matter in water" (UAC R317-6-1.11). This definition encompasses virtually anything that could be discharged from the landfill.

Protection levels for these contaminants must be met at a compliance monitoring point**.** Point of discharge "means the area within outermost location at which effluent or leachate has been stored, applied, disposed of, or discharged; for diked facilities, the outermost edge of the dikes" (UAC R317-6-1.28). The point of discharge, therefore, is similar in concept to the point of compliance defined in 40 CFR 192.

UAC 317-6 protection levels vary with the classification of the groundwater, which varies according to water quality and potential use. At the Monticello landfill site, the shallow groundwater contains Class II groundwater. *Such groundwater could be used for drinking or similar uses after conventional water treatment.*

(D) Landfill Requirements from the Utah Solid and Hazardous Waste Act

UAC R315-8 implements a Utah law that applies the provisions of RCRA at the State level. Because UAC R315-8 is at least equal to, and potentially more stringent than, the comparable RCRA regulations in 40 CFR 264, the Utah rule is considered the governing standard.

UAC R315-8 is most important as the source of design requirements for the landfill liner and cover. UAC R315-8-14.2 requires that the entire landfill cell must have a liner system, that the system must include two liners with a leachate collection and removal system above each liner, and that the lower liner must be a composite of a geomembrane and a clay layer. It also requires that the permeability of the clay layer be less than or equal to $1x10^{-7}$ cm/s (same value specified in RCRA regulations 40 CFR 264.301), which will be used in this study as a performance metric. The rule also provides for alternate design or operating practices if the owner or operator demonstrates functional equivalency (UAC R315-8-14.2(d)). UAC R315-8-14.3 sets requirements for monitoring and inspection of liner systems, both during and after construction.

(E) DOE Orders

Although not listed as an ARAR, the DOE, through a DOE "Order," sets standards for maximum doses to a member of the public from all routine DOE operations, including remedial actions.

3.2.4 Summary of Performance Metrics for the Monticello Repository

Each of the regulations discussed above was reviewed for quantitative performance objectives that govern the long-term performance of the mill tailings landfill/repository at Monticello. Table 1 summarizes these metrics. When two or more regulations set the same standard, only the standard set by 40 CFR 192 is presented in Table 1.

Of the metrics summarized in Table 1, only a few are used in this study as performance objectives for the selected scenarios (Section 4.1). In addition, the amount of percolation reaching the mill tailings is used as a performance objective based on the requirements in RCRA 40 CFR 264.301 and UAC R315-8-14.2. The performance objectives used in this study are summarized as follows:

(1) Percolation of water reaching mill tailings shall be less than $1x10^{-7}$ cm/s. This is based on the prescribed maximum conductivity of the clay liner in 40 CFR 264.301 and UAC R315-8-14.2, where a unit-gradient flow is assumed to equate percolation to conductivity.

(2) Average flux of radon-222 gas shall be less than 20 $pCi/m^2/s$ at the surface of the repository cover.

(3) Combined radium-226 and radium-228 concentrations in groundwater shall be less than 5 pCi/L (only radium-226 is evaluated in this study).

(4) The effective dose to a member of the public from all pathways shall be less than 100 mrem/year (only radium-226 is evaluated in this study).

Table 1. Summary of performance objectives applicable to the Monticello Mill Tailings Repository.

Media	Standard	Point of Compliance	Period of Compliance	Regulation
All Pathways	< 100 mrem/year Effective Dose Equivalent from all routine DOE activities	to a member of the public	not defined	DOE Order 5400.5 II 1. a.
Atmosphere	< 10 mrem/year Effective Dose Equivalent, excluding Rn	to a member of the public	not defined	40 CFR 61.92
Atmosphere	Average flux of Rn-222 < 20 pCi/m^2/second **or** (see next row)	In air above landfill, averaged over entire landfill	1,000 years if reasonably achievable, and, in any case, for at least 200 years	40 CFR 192.02(a) and 40 CFR 192(b)(1)
Atmosphere	annual average concentration of Rn-222 in air < 0.5 pCi/L	At or above any location outside the landfill	1,000 years if reasonably achievable, and, in any case, for at least 200 years	40 CFR 192.02(a) and 40 CFR 192(b)(2)
Groundwater	Arsenic < 0.05 mg/L[1, 2]	Intersection of vertical plane with uppermost aquifer at downgradient limit of disposal area plus area taken by dike or other waste barrier	1,000 years if reasonably achievable, and, in any case, for at least 200 years	40 CFR 192.02(a) and 40 CFR 192.02(c)(4) and Table 1 to Subpart A of 40 CFR 192
	Chromium < 0.05 mg/L[1, 2]			
	Lead < 0.05 mg/L[1, 2]			
	Molybdenum < 0.1 mg/L[1, 2]			
	Selenium < 0.01 mg/L[1, 2]			
	Combined Ra-226 & Ra-228 < 5 pCi/L[1, 2]			
	Combined U-234 & U-238 < 30 pCi/L[1, 2, 3]			
	Gross alpha-particle activity, excluding Rn and U < 15 pCi/L[1, 2]			
Groundwater	Beta particles, and photons from man-made radionuclides < 4 mrem/yr	in community water supply systems	not defined	40 CFR 141.16

[1] If background is below this level; [2] An alternative concentration limit may be established under 40 CFR 192.02 (c)(ii)(A); [3] Where secular equilibrium obtains, this criterion will be satisfied by a concentration of 0.044 milligrams per liter (0.044 mg/l). For conditions of other than secular equilibrium, a corresponding value may be derived and applied, based on the measured site-specific ratio of the two isotopes of uranium.

4. Performance Assessment of the Monticello Mill Tailings Repository

This section presents an illustration of the risk-based performance-assessment method (as defined in Section 2) for the Monticello Mill Tailings Repository Site. Scenarios are first developed based on relevant performance objectives (Section 3.2.4) and applicable features, events, and processes at the site. A total-system framework is then developed to integrate the more detailed "process models" in each scenario. Descriptions of each process model are provided along with the parameter distributions, and a discussion of the results of the simulated performance metrics is presented.

4.1 Scenario Development and Screening of FEPs

The first step in the performance assessment is to develop relevant scenarios based on performance objectives and applicable features, events, and processes at the site. The performance objectives have been summarized in Section 3.2.4, and a list of relevant features, events, and processes at the Monticello site are listed in Table 2 along with their treatment in this study. Rigorous methods have been developed by Cranwell et al. (1982) to identify and screen FEPs. However, the scoping nature of this assessment did not allow for a full implementation of the FEPs process. Therefore, only a subset of all possible FEPs were identified in Table 2 based on best professional judgment. In addition, only radium-226 (and its daughter products) was chosen as the aqueous contaminant of interest for transport via the groundwater, and radon-222 was chosen as the gas-phase contaminant of interest for gas transport to the surface of the cover. The inclusion of additional radionuclides may increase the peak concentrations and doses simulated in this assessment. A total of eight scenarios were chosen based on the relevant FEPs and performance objectives. Table 3 provides a summary and explanation of these scenarios.

Table 2. List of features, events, and processes relevant to the Monticello Mill Tailings Repository.

Title	Description	Treatment
Environmental Conditions		
Future climates	Future climates may yield different temperatures and precipitation rates than present conditions.	Included in HELP (Hydrologic Evaluation of Landfill Performance) model.[1]
Future vegetation	Vegetation on covers may change with future climates.	Included in HELP model.[1]
Erosion	Wind and flooding can cause erosion of soils, which may impact infiltration.	Not included. Uncertain impact.
Percolation to Waste		
Run-on/Run-off	Precipitation can run-on and run-off surfaces above the repository.	Included in HELP model.[1]
Evapo-transpiration	Precipitation can be evaporated and transpired by plants.	Included in HELP model.[1]
Storage	Infiltration can be stored in soils.	Included in HELP model.[1]
Capillary barriers/lateral diversion	Percolation can be diverted by capillary barriers.	Included in HELP model.[1]
Membrane leakage	Membranes and liners can leak if defects are present.	Included in HELP model.[1]
Membrane deterioration	Membranes and liners can deteriorate over time.	Included in HELP model using increased defects for future conditions.[1]

Title	Description	Treatment
Fast flow paths (e.g., root holes)	Heterogeneities in the cover may cause fast flow paths.	Not included. May have large impact.
Spatial and temporal variability in infiltration	Episodic infiltration and spatial variability may increase the infiltration in locations	Not included. May have large impact.
Source-Term Release and Transport through Cover		
Leaching	Radionuclides can leach into percolating pore water	Included in MEPAS source-term model.[3]
Radon gas flux	Radon gas can transport through the cover to the surface	Included in RAECOM model.[2]
Barometric pumping	Barometric pressure variations may cause advection of radon gas to the surface	Not included. May have large impact.
Subsidence of waste	Waste could subside and change shape of repository	Not included. Not expected to have a large impact.
Vadose-Zone Transport		
Advection	Radionuclides can transport in percolating pore water.	Included in MEPAS vadose-zone model.[4]
Diffusion/Dispersion	Radionuclides can transport by molecular and mechanical diffusion/dispersion.	Included in MEPAS vadose-zone model.[4]
Sorption	Radionuclides can adsorb onto solid surfaces.	Included in MEPAS vadose-zone model.[4]
Fast transport paths	Heterogeneities and colloids may facilitate faster transport	Not included. May have a large impact.
Water-table rise	Future wetter climates may cause the water table to rise, decreasing the vadose-zone transport distance	Not included. May have a large impact.
Saturated-Zone Transport		
Advection	Radionuclides can transport in groundwater.	Included in MEPAS saturated-zone model.[4]
Diffusion/Dispersion	Radionuclides can transport by molecular and mechanical diffusion/dispersion in groundwater.	Included in MEPAS saturated-zone model.[4]
Sorption	Radionuclides can adsorb onto solid surfaces.	Included in MEPAS saturated-zone model.[4]
Fast transport paths	Heterogeneities and colloids may facilitate faster transport	Not included. May have a large impact.
Human Exposure		
Shallow alluvial aquifer	Humans can use water from the shallow alluvial aquifer for agriculture	Included in MEPAS exposure, intake, and health-impact models.[5]
Deep Burro Canyon aquifer	Humans can use water from the deep aquifer for agriculture and consumption.	Included in MEPAS exposure, intake, and health-impact models.[5]
Inhalation	Humans can inhale radon gas and contaminated particulates.	Not included. Not expected to have a large impact.
Direct contact	Humans can experience dermal contact through bathing, swimming, etc.	Not included. Not expected to have a large impact.
Disruptive Events		
Earthquakes, tornadoes, human intrusion, bio-intrusion	These events could disrupt the repository site and cause changes to transport processes and pathways	Not included. May have a large impact.

[1]Schroeder et al. (1994a,b); [2]Rogers et al. (1984); [3]Streile et al. (1996); [4]Whelan et al. (1996); [5]Strenge and Chamberlain (1995)

Table 3. Summary of scenarios and performance objectives evaluated in this study.

Senario	Description	Climate	Performance Objective Addressed
1	Infiltration percolates through the cover and reaches the mill tailings.	Present	• Percolation of water reaching mill tailings shall be less than $1x10^{-7}$ cm/s.

Senario	Description	Climate	Performance Objective Addressed
2	Infiltration percolates through the cover and reaches the mill tailings.	Future	• Percolation of water reaching mill tailings shall be less than $1x10^{-7}$ cm/s.
3	Radon-222 gas diffuses from the mill tailings to the surface.	Present	• Average flux of radon-222 gas shall be less than 20 pCi/m^2/s at the surface of the repository cover.
4	Radon-222 gas diffuses from the mill tailings to the surface.	Future	• Average flux of radon-222 gas shall be less than 20 pCi/m^2/s at the surface of the repository cover.
5	Radium-226 leaches from the mill tailings and transports through the composite liner, the vadose zone, and into the shallow alluvial aquifer where water is used for agricultural purposes.	Present	• Radium-226 concentration in groundwater shall be less than 5 pCi/L. • The effective dose to a member of the public from all pathways shall be less than 100 mrem/year.
6	Radium-226 leaches from the mill tailings and transports through the composite liner, the vadose zone, and into the shallow alluvial aquifer where water is used for agricultural purposes.	Future	• Radium-226 concentration in groundwater shall be less than 5 pCi/L. • The effective dose to a member of the public from all pathways shall be less than 100 mrem/year.
7	Radium-226 leaches from the mill tailings and transports through the composite liner, the vadose zone, and into the deep Burro Canyon aquifer where water is used for agricultural purposes and drinking.	Present	• Radium-226 concentration in groundwater shall be less than 5 pCi/L. • The effective dose to a member of the public from all pathways shall be less than 100 mrem/year.
8	Radium-226 leaches from the mill tailings and transports through the composite liner, the vadose zone, and into the deep Burro Canyon aquifer where water is used for agricultural purposes and drinking.	Future	• Radium-226 concentration in groundwater shall be less than 5 pCi/L. • The effective dose to a member of the public from all pathways shall be less than 100 mrem/year.

Once the scenarios were developed, conceptual models of the features, events, and processes for each scenario could be formulated. The conceptualizations involve simplifications of the complex nature of the site, but they capture the salient features to be modeled. The conceptual models include contaminant source and release information (as applicable), a description of transport mechanisms and pathways, and a definition of modeling endpoints. Figure 5**,** Figure 6, and Figure 7 illustrate the conceptual models of the various scenarios (see Table 3). From a computational standpoint, each scenario is simulated stochastically and independently to yield distributions of the corresponding performance metrics in Table 3. Fault trees or other analysis methods could be used to assign probabilities to each scenario and combine these distributions, but for this example, each scenario is treated independently.

Figure 5 illustrates the conceptualization for scenarios 1-4 for water and gas transport through the landfill cover for both present and future conditions. Under future conditions, additional uncertainty is added to parameters such as precipitation and liner quality to reflect potentially wetter conditions and deteriorated materials. Figure 6 illustrates scenarios 5 and 6, where radium-226 (and its daughter products Rn-222, Pb-210, Bi-210, and Po-210) leach from the mill

tailings and transport to the shallow alluvial aquifer under present and future conditions. Figure 7 illustrates scenarios 7 and 8, which are similar to scenarios 5 and 6 except the aquifer is thicker and located more deeply in the Burro Canyon. In addition, the water from the Burro Canyon aquifer is used for both drinking and agriculture, whereas the water from the shallow alluvial aquifer is used only for agriculture. Transport to both the shallow alluvial aquifer and the Burro Canyon aquifer could not be simulated simultaneously because of limitations in the FRAMES model, but because the transport the Burro Canyon aquifer is much longer, the combined peak concentration and dose are not expected to be significantly different than the results from the shallow alluvial aquifer. More details regarding the various conceptual and process models used in the simulations are provided in Section 4.3.

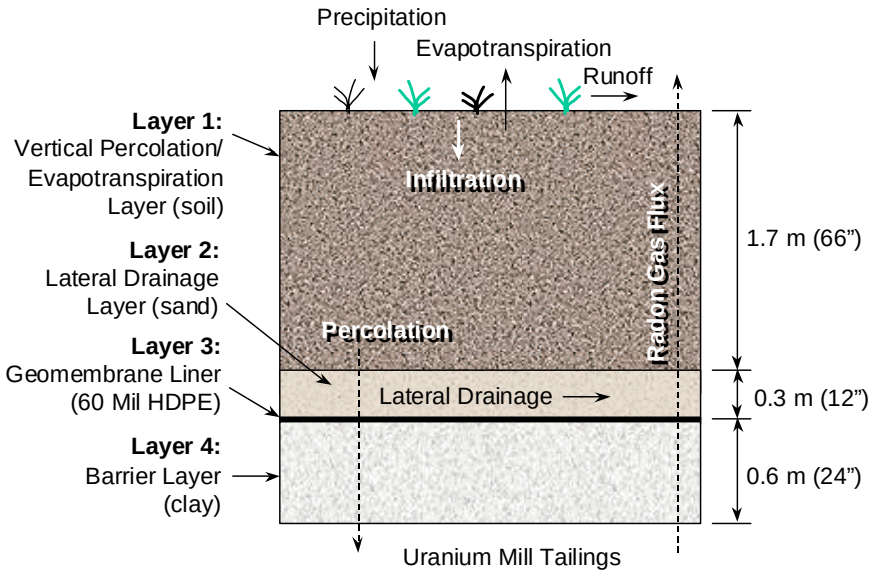

Figure 5. Conceptual model for percolation (scenarios 1 and 2) and gas transport (scenarios 3 and 4) through the cover for present and future conditions. A 3% slope is assumed for the drainage layer.

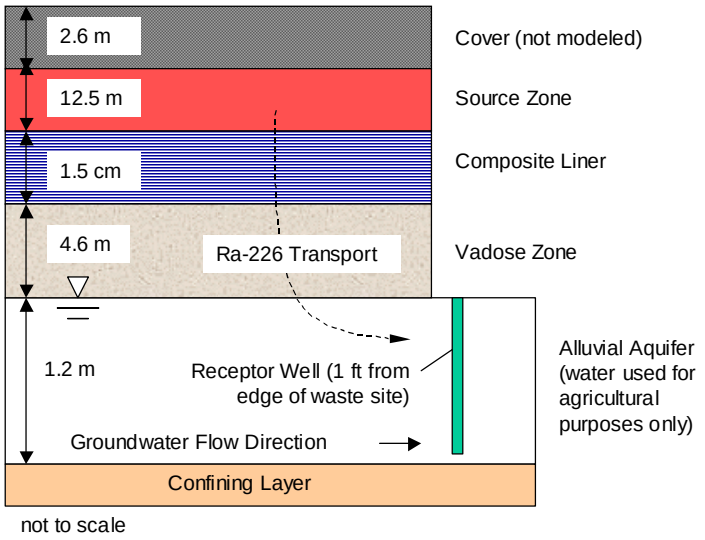

Figure 6. Conceptual model for radionuclide transport from the mill tailings to the shallow alluvial aquifer and location of receptor well for present (scenario 5) and future (scenario 6) conditions.

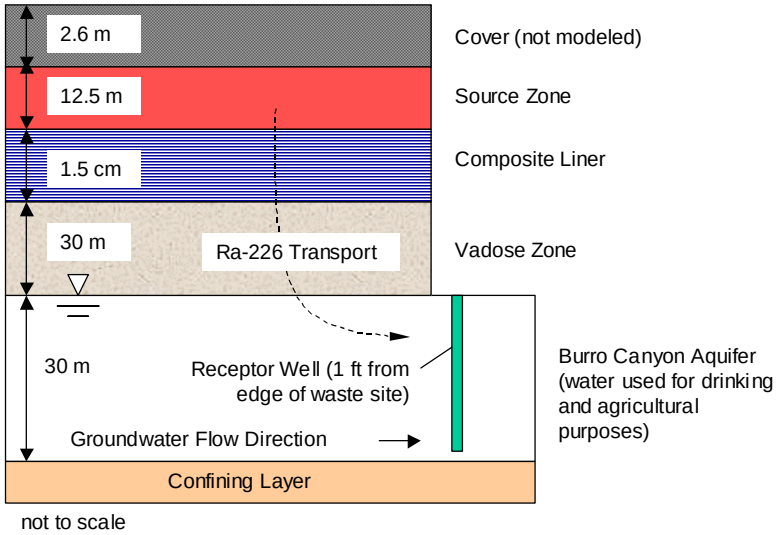

Figure 7. Conceptual model for radionuclide transport from the mill tailings to the deep Burro Canyon aquifer and location of receptor well for present (scenario 7) and future (scenario 8) conditions.

4.2 Total-System Framework Model

Each scenario contains a combination of models that represent processes in different media (e.g., transport in the vadose zone, saturated zone, air, etc.). Often, these models do not originate from the same numerical code, and a framework is required to seamlessly integrate individual codes into a multimedia assessment. The system used for this study was the Framework for Risk Analysis in Multimedia Environmental Systems (FRAMES). FRAMES was developed by Pacific Northwest National Laboratory (PNNL) with funding from DOE and EPA. The FRAMES system allows for a holistic approach to modeling in which models of different type (i.e., source, fate and transport, exposure, health impact), resolution (i.e., analytical, semi-analytical, and numerical), and operating platforms can be combined as part of the overall assessment of contaminant fate and transport in the environment. The FRAMES system provides a user-friendly platform for integrating medium specific computer models, an extensive and editable contaminant database, a powerful and flexible sensitivity/uncertainty module, and textual and graphical viewers for presenting modeling outputs. The FRAMES system employs a graphical user interface (GUI) that aids a user in setting up and simulating each conceptual site model. Screen captures from the GUI can also be very helpful as a tool to communicate the assessment approach to others. Figure 8 presents a screen capture of the FRAMES GUI depicting scenario 5 in this study. Similar cases were set up in FRAMES for the other scenarios in this study; however, scenarios 1 and 2 were simulated separately using HELP v. 3.07 (Schroeder et al., 1994a,b) because HELP is not yet currently integrated with FRAMES.

The module icons displayed in Figure 8 represent detailed process models that can be accessed by clicking on the icon. Existing models in FRAMES include those derived from the Multimedia Environmental Pollutant Assessment System (MEPAS) (Whelan et al., 1992). MEPAS is a physics-based environmental analysis code that integrates source-term, transport, and exposure models for endpoints such as concentration, dose, or risk. As its name suggests, MEPAS is capable of computing contaminant fluxes for multiple routes, which include leaching to groundwater, overland runoff, volatilization, suspension, radioactive decay, constituent degradation, and source/sink terms. The radioactive-decay loss route is always utilized for radionuclides; it cannot be turned off. The model also requires the user to select from three different source medias: surface soil, surface water/pond, and contaminated aquifer. Section 4.3 provides more detailed discussion of each process model used in the scenarios.

In Figure 8, the arrows on the screen linking the icons from the Monticello Landfill icon to the Health Impacts icon indicate the direction of data flow through the system. Additional arrows originating from the FRAMES contaminant database (con1) indicate that all modules are receiving contaminant data. Finally, arrows linking module icons to the Sensitivity Model icon indicate those modules that contain stochastic parameters.

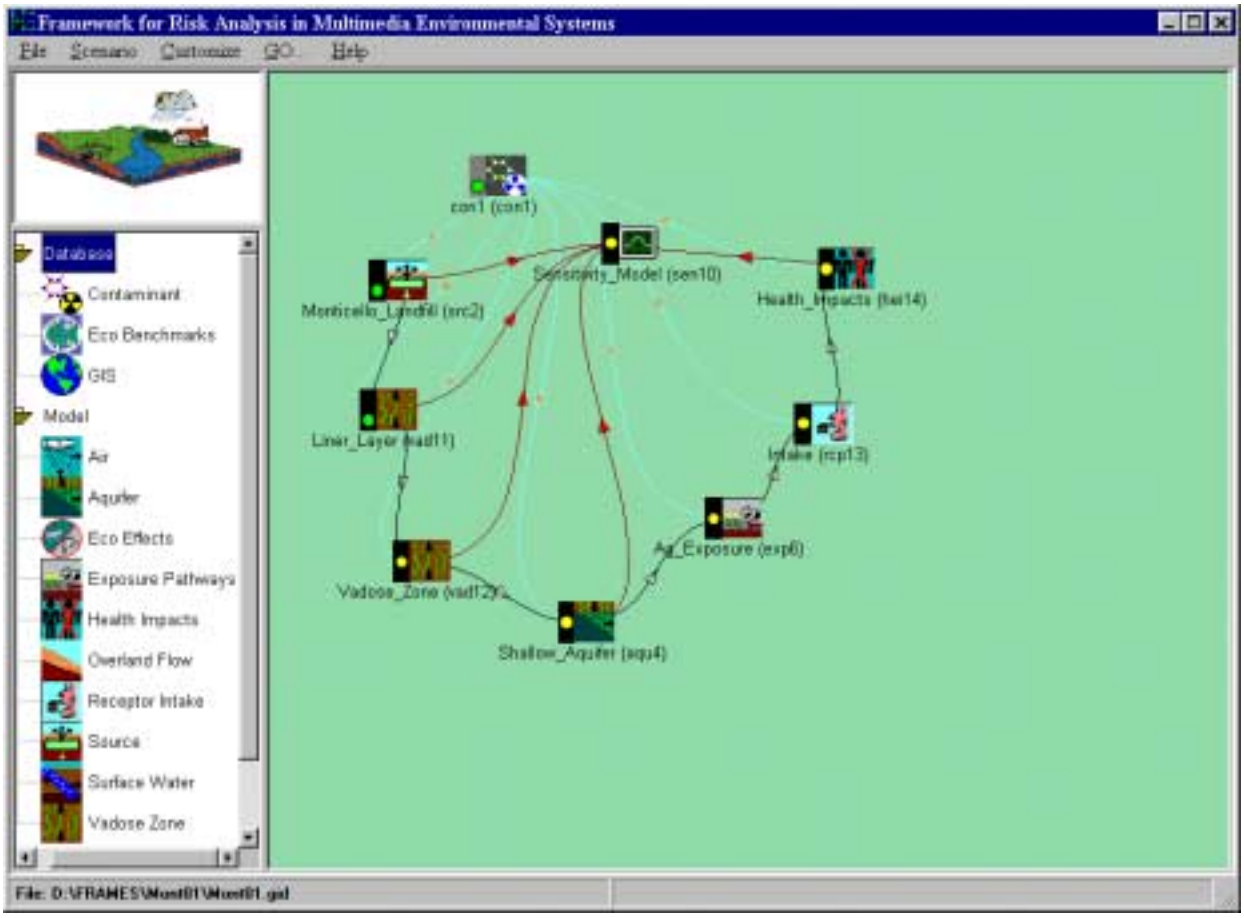

Figure 8. Screen capture of FRAMES graphical user interface for scenario 5.

In most modeling exercises there are uncertainties associated with each input parameter. Uncertainty analyses are performed in an effort to try to capture the effect of parameter uncertainty and variability on the simulated results. Invariably, certain parameters impact modeling results more than others when their values are changed. However, in most cases, this type of behavior is difficult to predict when a modeling scenario includes multiple models and multiple uncertain input parameters. For this reason, FRAMES allows parameters to be varied stochastically, and it records the sampled parameter values for each realization so that they can be used in subsequent sensitivity analyses. The sensitivity/uncertainty module in FRAMES is called the Sensitivity Uncertainty in Multimedia Modeling Module (SUMMM). The SUMMM module can be attached to any model that has been integrated into FRAMES and allows the user to stochastically vary any input parameter that is identified in the process models. Input parameters can be stochastically varied by a distribution, correlation coefficient, an equation, or any combination of these three options. Four distributions are currently available: (1) uniform, (2) log uniform, (3) normal, and (4) log normal. SUMMM utilizes the Latin Hypercube Sampling (Wyss and Jorgensen, 1998) technique to minimize the number of modeling runs that must be performed to accurately represent distributions selected by the user.

The stochastic parameters that were varied in each scenario are detailed in Section 4.3. One hundred realizations were simulated in each scenario (except for scenarios 1 and 2) using FRAMES with the SUMMM module. In scenarios 1 and 2, only 50 realizations were simulated because the HELP code was not integrated with FRAMES and had to be run manually for each realization (current efforts are underway to integrate HELP with FRAMES so that multiple stochastic simulations can be automated). The results of each simulation that were recorded correspond to the performance metrics listed in Table 1.

4.3 Process-Model Development and Parameter Distributions

This section presents the detailed process models that were integrated in the total-system model FRAMES. An overview of the model is provided along with the necessary input parameter distributions for the following process models: (1) water percolation through the cover; (2) radon gas transport through the cover; (3) source-term release; (4) vadose-zone transport; (5) saturated-zone transport; and (6) human exposure.

4.3.1 Water Percolation through the Cover

Water percolation through the cover to the waste is affected by numerous factors including the weather, plant behavior, and the properties of the cover systems and their variability. The HELP v. 3.07 code (Schroeder et al., 1994a,b) considers the above variables for landfill cover systems. The processes modeled in HELP include weather, snowmelt, runoff, infiltration, evapotranspiration, vegetative growth, soil moisture storage, lateral subsurface drainage, leachate recirculation, unsaturated vertical drainage, and leakage through soil, geomembrane or composite liners. HELP is widely used due to its ease of use compared to other numerical codes and its acceptance within the regulatory community. Convenient default parameters are included for soils, geosynthetic materials, evapotranspiration processes, and weather parameters. Thus, the user-input parameters can be minimal. However, it uses a simplified water routing technique to evaluate the distribution of water in the landfill covers, and flow due to capillary pressure gradients, which may be important in semi-arid and arid environments, is neglected. As a result, the HELP model of flow through the cover does not account for capillary barriers (i.e., between layers 1 and 2), but it does allow for lateral drainage in layer 2, which is assumed to have a 3% slope. This simplification can lead to overprediction of percolation/leakage in semi-arid and arid conditions (Fleenor and King, 1995; Webb et al., 1997).

A number of other codes include more mechanistic models for unsaturated flow; however, other features important to landfill covers are not included. For example, TOUGH2 (Pruess et al., 1991) has a much more comprehensive model for unsaturated flow including local heterogeneity as demonstrated by Ho and Webb (1998) for capillary barriers, but the effect of weather and plants is not included. UNSAT-H (Fayer, 2000) is another candidate code. While it does include some weather and plant features, it is restricted to one-dimensional geometry. In the interest of trying to include the relevant features, events and processes, the HELP code was chosen for the present scenario analysis. However, future model development in this area might be needed in order to adequately capture all the necessary physics.

Parameter values for the HELP model of percolation through the landfill cover at the Monticello site were assigned based on site-specific data, where available, and on general information about soil characteristics in other cases. Sensitivity analyses were conducted with the HELP model to provide information on parameter sensitivity and to determine which parameters should be included as stochastic parameters in the performance-assessment analyses. Uncertainties in key parameters and correlations were quantitatively evaluated and uncertainty distributions were assigned.

Sensitivity analyses with the HELP model of the landfill cover were conducted using the expected values of model parameters (Abraham and Waugh, 1995) and varying individual parameters within reasonable ranges for present conditions (see Apendix A for details). Average monthly precipitation and temperature data for Monticello, Utah, were used in the model (Owenby and Ezell, 1992). The dependent variable in sensitivity analyses was the average annual percolation through the landfill cover. Analysis of environmental factors indicated moderate sensitivity to total precipitation, evaporative zone depth, and maximum leaf-area index. Results also indicated moderate to high sensitivity to the saturated hydraulic conductivity, wilting point, and field capacity in layer 1 and moderate sensitivity to the saturated hydraulic conductivity, wilting point, and field capacity in layer 2 (see Figure 5 for layer configuration). Results for the geomembrane (layer 3) indicated moderate sensitivity to defect density and placement quality. Moderate sensitivity to saturated hydraulic conductivity was observed for layer 4. Note that the definitions for these parameters can be found in Schroeder et al. (1994a,b). The results of the sensitivity analyses were used as a semi-quantitative basis for choosing the parameters to be treated stochastically in the analyses of percolation with the HELP model. Distributions for uncertain parameters are summarized in Table 4 for present (scenario 1) and future (scenario 2) climatic conditions, and brief descriptions of the distributions are provided below.

The upper bound of the evaporative-zone-depth parameter for layer 1 is the total thickness of the layer and the lower bound is specified as 0.81 m (32 in) based on professional judgment. A uniform distribution is specified for the evaporative-zone-depth parameter, based on the lack of specific information on the relative probability of the value. The maximum leaf-area index is assigned a uniform uncertainty distribution with a lower bound of 0.0 (corresponding to no vegetation) and an upper bound of 1.6 for present climatic conditions and 2.0 for future climatic conditions (Waugh, personal communication, 2001).

Uncertainty in the hydraulic parameters for layer 1 in the landfill cover was analyzed based on data from the site (Daniel B. Stephens and Associates, 1993). Soil drainage data were fit using the van Genuchten model for soil characteristics for eight samples. Results were converted to the field capacity and wilting point of the Brooks-Corey model for input to the HELP code. Statistical analysis indicated an approximate log-normal distribution of saturated hydraulic conductivity, when a single outlier in the data set was discarded. The distributions of field capacity and wilting point are approximately uniform and the lowest and highest observed values of these parameters were taken as bounds to uniform distributions. See Appendix A for more details.

Uncertainty in the hydraulic parameters for layers 2 and 4 was evaluated based on a compilation of data for sand and clay, respectively (Carsel and Parrish, 1988). This approach was taken

because site-specific data were not available for these materials. The uncertainty distributions given for saturated hydraulic conductivity and the van Genuchten soil characteristic parameters in Table 4 were back-transformed from the distributions provided in Carsel and Parrish (1988). The van Genuchten parameters were converted to the Brooks-Corey parameters of field capacity and wilting point for use in the HELP model. See Appendix A for more details.

Stochastic parameters related to the geomembrane (layer 3) are the defect density and the placement quality. For present conditions, the uncertainty distribution for the defect density was designated as a normal distribution with a mean of 0.0012 defects/m^2 (5 defects/acre) and the standard deviation was set at $3.7x10^{-4}$ defects/m^2 (1.5 defects/acre) to give an approximate variation from 0 to 0.0025 defects/m^2 (0 to 10 defects/acre), based on professional judgment. Degradation of the geomembrane was incorporated into the probabilistic analyses by varying the defect density for future conditions in a uniform distribution between 0 defects/m^2 (0 defects/acre) and 1.2 defects/m^2 (5000 defects/acre), corresponding to essentially complete degradation of the plastic geomembrane. A uniform distribution in the placement quality from 1 to 6 (perfect placement to worst-case placement) was assigned, given the lack of site-specific information on placement quality (see Shroeder et al., 1994a,b for details).

Uncertainty in precipitation and temperature for future climatic conditions was incorporated in the analyses by defining parameters for the precipitation multiplier and temperature adjustment relative to present conditions. The precipitation multiplier is the ratio of the average annual precipitation for future conditions to the present annual average. The precipitation multiplier was assigned a uniform distribution with 1.0, corresponding to present conditions, as a lower bound. The upper bound of 2.04 was specified to correspond to the ratio of estimated glacial climatic precipitation of 80 cm/year (Waugh and Petersen, 1994) to present average annual precipitation of 39.3 cm/year (Owenby and Ezell, 1992). The precipitation multiplier was applied to the individual monthly average precipitation values used in the HELP model for the simulations of future conditions. A uniform uncertainty distribution for the average temperature adjustment was specified with a lower bound of –6.0 ^oC and an upper bound of 0.0 ^oC. The lower bound corresponds to the estimated average annual temperature for cooler, glacial climatic conditions (Waugh and Petersen, 1994). The value of the temperature adjustment was added to the average monthly temperature values (present conditions) used in the HELP model for simulations of future conditions (Owenby and Ezell, 1992).

Table 4. Uncertainty distributions for stochastic parameters in the percolation model.

Layer	Parameter	Uncertainty Distribution (Present Conditions)	Uncertainty Distribution (Future Conditions)
1	Evaporative Zone Depth (m)	Uniform Distribution Lower Bound: 0.81 Upper Bound: 1.8	Uniform Distribution Lower Bound: 0.81 Upper Bound: 1.8
1	Maximum Leaf-Area Index	Uniform Distribution Lower Bound: 0.0 Upper Bound: 1.6	Uniform Distribution Lower Bound: 0.0 Upper Bound: 2.0
1	Effective Saturated Hydraulic Conductivity (cm/s)	Log Normal Distribution Geometric Mean: $3.0x10^{-4}$ Geometric S.D.: 8.9	Log Normal Distribution Geometric Mean: $3.0x10^{-4}$ Geometric S.D.: 8.9
1	Field Capacity	Uniform Distribution Lower Bound: 0.22 Upper Bound: 0.38	Uniform Distribution Lower Bound: 0.22 Upper Bound: 0.38

Layer	Parameter	Uncertainty Distribution (Present Conditions)	Uncertainty Distribution (Future Conditions)
1	Wilting Point	Uniform Distribution Lower Bound: 0.08 Upper Bound: 0.21	Uniform Distribution Lower Bound: 0.08 Upper Bound: 0.21
2	Effective Saturated Hydraulic Conductivity (cm/s) [1]	Log Ratio Normal Distribution Mean: -3.94 S.D.: 1.15	Log Ratio Normal Distribution Mean: -3.94 S.D.: 1.15
2	Van Genuchten Alpha (1/cm) [1]	Log Ratio Normal Distribution Mean: 0.378 S.D.: 0.439	Log Ratio Normal Distribution Mean: 0.378 S.D.: 0.439
2	Van Genuchten N [1]	Log Normal Distribution Geometric Mean: 2.66 Geometric S.D.: 1.11	Log Normal Distribution Geometric Mean: 2.66 Geometric S.D.: 1.11
3	Defect Density ($1/m^2$)	Normal Distribution Mean: 0.0012 S.D.: $3.7x10^{-4}$	Uniform Distribution Lower Bound: 0 Upper Bound: 1.2
3	Placement Quality	Uniform Distribution Lower Bound: 1 Upper Bound: 6	Uniform Distribution Lower Bound: 1 Upper Bound: 6
4	Effective Saturated Hydraulic Conductivity (cm/s) [2]	Log Ratio Normal Distribution Mean: -5.75 S.D.: 2.33	Log Ratio Normal Distribution Mean: -5.75 S.D.: 2.33
4	Van Genuchten Alpha (1/cm) [2]	Log Ratio Normal Distribution Mean: -4.145 S.D.: 1.293 Lower Bound: -5.01 Upper Bound: 0.912	Log Ratio Normal Distribution Mean: -4.145 S.D.: 1.293 Lower Bound: -5.01 Upper Bound: 0.912
4	Van Genuchten N [2]	Log Normal Distribution Geometric Mean: 1.00 Geometric S.D.: 1.13 Lower Bound: 0.0 Upper Bound: 0.315	Log Normal Distribution Geometric Mean: 1.00 Geometric S.D.: 1.13 Lower Bound: 0.0 Upper Bound: 0.315
N/A	Precipitation Multiplier	N/A	Uniform Distribution Lower Bound: 1 Upper Bound: 2.04
N/A	Average Temperature Adjustment (^oC)	N/A	Uniform Distribution Lower Bound: -6.0 Upper Bound: 0.0

[1]see Carsel and Parrish (1988) parameter distributions for sand.; [2]see Carsel and Parrish (1988) parameter distributions for clay; N/A: Not Applicable; S.D.: Standard Deviation

Important correlations exist between several of the uncertain parameters in the HELP model for percolation at the Monticello site. The correlation coefficients (R-values) for these correlations are summarized in Table 5. The correlation between evaporative-zone depth and maximum leaf-area index was based on professional judgment that higher plant density would correspond to deeper rooting depth. The correlations between the hydraulic parameters in layer 1 were based on statistical analysis of site-specific data (Daniel B. Stephens and Associates, 1993). The values of the correlation coefficients for the hydraulic parameters in layers 2 and 4 were taken from Carsel and Parrish (1988). The moderate positive correlation between maximum leaf-area index and the precipitation multiplier for future conditions was based on professional judgment that wetter climatic conditions would generally correspond to higher plant density. The moderate negative correlation between the precipitation-multiplier parameter and the average temperature adjustment was based on professional judgment that wetter climatic conditions would generally correspond to lower average temperatures.

Table 5. Correlation coefficients between parameters in the percolation model.

Parameter 1	Parameter 2	Correlation Coefficient (Present Conditions)	Correlation Coefficient (Future Conditions)
Evaporative Zone Depth (inches)	Maximum Leaf-Area Index	0.60	0.60
Effective Saturated Hydraulic Conductivity (cm/s) (layer 1)	Field Capacity (layer 1)	-0.66	-0.66
Field Capacity (layer 1)	Wilting Point (layer 1)	0.88	0.88
Effective Saturated Hydraulic Conductivity (cm/s) (layer 2)	Van Genuchten Alpha[1] (1/cm) (layer 2)	0.743	0.743
Effective Saturated Hydraulic Conductivity (cm/s) (layer 2)	Van Genuchten N[1] (layer 2)	0.843	0.843
Van Genuchten Alpha[1] (1/cm) (layer 2)	Van Genuchten N (layer 2)	0.298	0.298
Effective Saturated Hydraulic Conductivity (cm/s) (layer 4)	Van Genuchten Alpha (1/cm) (layer 4)[1]	0.948	0.948
Effective Saturated Hydraulic Conductivity (cm/s) (layer 4)	Van Genuchten N[1] (layer 4)	0.908	0.908
Van Genuchten Alpha[1] (1/cm) (layer 4)	Van Genuchten N[1] (layer 4)	0.910	0.910
Maximum Leaf-Area Index	Precipitation Multiplier	N/A	0.60
Precipitation Multiplier	Average Temperature Adjustment (^{o}C)	N/A	-0.60

[1]Van Genuchten parameters were transformed to wilting point and field capacity for use in HELP (assumes wilting point and field capacity occur at 15.3 m (15 bars) and 3.37 m (0.33 bars) of head at 20^{o}C, respectively); N/A: Not Applicable

Multiple realizations of the uncertain parameter values were generated using the Latin Hypercube sampling method for input to the HELP percolation model. The Latin Hypercube stratified sampling algorithm provides an efficient method of sampling for uncertainty assessment that preserves the correlations specified among parameters. The uncertainty distributions and correlation coefficients given in Table 4 and Table 5 were specified in the input to the Latin Hypercube sampling. The LHS computer code (Wyss and Jorgensen, 1998) was used to produce 50 realizations of uncertain parameter values for present conditions (scenario 1) and 50 realizations for future conditions (scenario 2).

4.3.2 Radon Gas Transport through the Cover

One objective of the cover design is attenuation of the radon emanation from the mill tailings to the atmosphere at the Monticello site. The landfill cover acts as a gas diffusion barrier, allowing time for the decay of the relatively short-lived Rn-222 gas (half-life = 3.8 days) during migration through the pore spaces of the cover soil. In particular, the compacted clay layer of the cover design serves as a barrier to radon migration due to its relatively low diffusion coefficient. Regulatory requirements limit the allowable flux of Rn-222 from the waste to the land surface to 20 pCi/m^{2}·s.

The conceptual model of radon migration through the landfill cover is one-dimensional upward transport driven by the difference in concentration in the tailings and the atmosphere. The processes affecting transport are molecular diffusion and radioactive decay. The boundary conditions for the problem are defined by a specified production rate of radon in the mill tailings and the assumption of zero radon concentration in the air at the land surface. Steady-state conditions, with regard to the radon concentration profile and flux, are also assumed to exist. Formulation of the radon gas transport model for present (scenario 3) and future (scenario 4) climatic conditions are presented below.

The mathematical model for steady-state one-dimensional transport of radon is expressed in the following equation:

$$D\frac{d^2C}{dx^2} - \lambda C + \frac{R\rho\lambda E}{\phi} = 0 \qquad (1)$$

where D is the effective diffusion coefficient for radon, C is the radon concentration in the pore space, λ is the decay constant of Rn-222, R is the specific activity of ^{226}Ra in the soil, ρ is the dry bulk density of the soil, E is the radon emanation coefficient, and ϕ is the total porosity of the soil.

The RAECOM computer code (Rogers et al., 1984) is used to solve this equation for the radon flux at the land surface. This program provides a solution for radon transport through a multi-layer landfill cover in which the material properties vary among the layers. The relevant properties for the materials in the cover are the thickness of the layer, the effective diffusion coefficient, porosity, moisture content, and radon emanation rate. Comparison between the RAECOM computer code and the RADON computer code (NRC, 1989) for an identical sample problem presented in the documentation of both codes indicates that the same solution is obtained from both codes.

Parameter values for the materials in the landfill cover at the Monticello site are assigned a representative value in some cases and are treated as stochastic parameters for those parameters exhibiting significant variability and sensitivity. Parameter values and uncertainty distributions used in the performance assessment of the landfill cover are summarized in Table 6 for present conditions and in Table 7 for future conditions. Deterministic parameters are those for which a single value is presented in the tables. Values defining the uncertainty distributions for stochastic parameters are presented in the tables for those parameters.

Table 6. Parameter values for radon flux model (present conditions).

Layer #[1]	Layer Thickness (cm)	Diffusion Coefficient (cm^2/s)	Porosity	Moisture Content (weight %)	Radon Emanation (pCi/cm^3-s)
5 (mill tailings)	1500.	Geometric Mean 1.49E-2 S.D. log 0.25	.43	Mean 4.8 S.D. 0.91	Mean 1.72E-3 S.D. 2.86E-4
4	61.	Geometric Mean 2.05E-3 S.D. log 0.25	.35	Mean 10.1 S.D. 0.91	0.
3	0.15	Mean 2.72E-5	.01	1.0	0.

Layer #[1]	Layer Thickness (cm)	Diffusion Coefficient (cm^2/s)	Porosity	Moisture Content (weight %)	Radon Emanation (pCi/cm^3-s)
		S.D. 8.15E-6			
2	30.	Geometric Mean 2.20E-2 S.D. log 0.25	.37	Mean 10.0 S.D. 0.91	0.
1	168.	Geometric Mean 1.08E-2 S.D. log 0.25	.43	Mean 10.1 S.D. 0.91	0.

[1]See Figure 5 for layer configuration.

Table 7. Parameter values for radon flux model (future conditions).

Layer #[1]	Layer Thickness (cm)	Diffusion Coefficient (cm2/s)	Porosity	Moisture Content (%)	Radon Emanation (pCi/cm3-s)
5 (mill tailings)	1500.	Geometric Mean 1.49E-2 S.D. log 0.25	.43	Mean 7.0 S.D. 2.10	Mean 1.72E-3 S.D. 2.86E-4
4	61.	Geometric Mean 2.05E-3 S.D. log 0.25	.35	Mean 10.1 S.D. 2.10	0.
3	0.15	Lower Bound 5.44E-6 Upper Bound 2.20E-2	.01	1.0	0.
2	30.	Geometric Mean 2.20E-2 S.D. log 0.25	.37	Mean 10.0 S.D. 2.10	0.
1	168.	Geometric Mean 1.08E-2 S.D. log 0.25	.43	Mean 10.1 S.D. 2.10	0.

[1]See Figure 5 for layer configuration.

The radon transport model consists of five layers, in which layer one consists of the uranium mill tailings. The other layers correspond to the layers in the landfill cover design used as the basis for the performance assessment analyses (see Figure 5). The thickness of each layer is fixed for this analysis of radon release to the atmosphere and is based on the cover design. The thickness of the tailings is based on an engineering estimate from the repository geometry (DOE, 1995). The porosity of each layer is the expected value of total porosity, as utilized in the analysis of groundwater percolation to the waste and from DOE (1995) for the tailings. The radon source term for layers above the tailings is set to zero because the regulatory limits placed on radon flux apply only to the tailings as a source and not to the background radon emanations from native materials at the site.

A log-normal uncertainty distribution is assigned to the diffusion coefficient in layers 1, 2, 4 and 5 (where layer 5 is the mill tailings). The geometric mean for the diffusion coefficient is taken from DOE (1995). The standard deviation of the log diffusion coefficient of 0.25 is based on the observation that measured values of the diffusion coefficient exhibit about one order of magnitude variability at intermediate values of moisture content (Rogers et al., 1984). The

geometric mean plus or minus two standard deviations of 0.25 results in an approximate variability of one order of magnitude for the diffusion coefficients in the realizations.

The distribution of the effective diffusion coefficient in the geomembrane (layer 3) is based on the following approximation. It is assumed that the diffusion coefficient for the intact high-density polyethylene is essentially zero. The uncertainty distribution for the defect density is the same as that used for the groundwater percolation analysis (i.e., normal distribution with a mean of 1.2×10^{-3} defects/m^2 (5 defects/acre) and a standard deviation of 3.7×10^{-4} defects/m^2 (1.5 defects/acre) for present conditions and a uniform distribution from 2.4×10^{-4} defects/m^2 (1 defect/acre) to 1.2 defects/m^2 (5000 defects/acre) for future conditions. It is assumed that each defect in the geomembrane is 1 cm^2 and will have a diffusion coefficient equal to the expected value for the overlying sand layer. In addition, each defect represents an effective area for diffusion of 1 m^2 through the geomembrane to account for multidimensional focusing of diffusion through the defect. The effective diffusion coefficient of the entire geomembrane is the area-weighted average diffusion coefficient, taking into account the total number of defects/m^2. This approach results in a normal distribution of the effective diffusion coefficient under present conditions (scenario 3). For future conditions (scenario 4), a uniform uncertainty distribution results, in which the diffusion coefficient varies from a very low value to a value that corresponds to essentially complete degradation of the geomembrane.

The uncertainty in the moisture content of the layers in the model is based on the analysis of percolation flux through the cover. The steady-state groundwater flux in the vadose zone, assuming a unit hydraulic gradient, is related to the moisture content by the following relationship in the van Genuchten model:

$$\frac{K(\theta)}{K_s} = \left(\frac{\theta - \theta_r}{\phi - \theta_r}\right)^{\frac{1}{2}} \left\{1 - \left[1 - \left(\frac{\theta - \theta_r}{\phi - \theta_r}\right)^{\frac{1}{m}}\right]^m\right\}^2 \qquad (2)$$

where $K(\theta)$ is the unsaturated hydraulic conductivity (equal to the flux for a unit gradient), K_s is the saturated hydraulic conductivity, θ is the volumetric moisture content, θ_r is the residual moisture content, ϕ is the porosity, and m is equal to (n-1)/n, where n is the van Genuchten fitting parameter. This expression was used to determine the corresponding value of moisture content in the tailings for each realization of percolation flux in the analysis (see Section 4.3.1), based on representative values of saturated hydraulic conductivity, residual moisture content, porosity, and van Genuchten n (Morrison et al., 1995). The resulting distribution of volumetric moisture content in the tailings for present conditions (scenario 3) has a mean of 7.2% and a standard deviation of 1.36%. The corresponding distribution for future conditions (scenario 4) has a mean of 10.5% and a standard deviation of 3.15%. These values of volumetric moisture content must be converted to weight % for input to the RAECOM program. Volumetric moisture content is converted to weight % moisture content by multiplying by the ratio of the density of water to the dry bulk density. Using a value of 1.50 g/cm^3 for bulk density results in the values shown in Table 6 and Table 7 for the uncertainty distributions for layer 5 (mill tailings).

The uncertainty in moisture content in the layers above the tailings cannot be directly derived in a similar manner because the average percolation flux in these layers was not calculated in HELP. It is assumed for these layers that the means of the distributions for moisture content are equal to the expected values for those layers and the standard deviation is the same as that derived for the tailings.

Measurements of effective diffusion coefficient at different levels of moisture saturation indicate a negative correlation between diffusion coefficient and moisture content (Rogers et al., 1984). For the analysis of radon gas transport in this study, a correlation coefficient of –0.7 was assumed between diffusion coefficient and moisture content for each layer (except the geomembrane). This correlation is qualitatively consistent with data presented for medium to medium-low values of moisture saturation (Rogers et al., 1984).

The radon source term from the tailings is a stochastic parameter with a mean value of 0.00172 pCi/cm^3-s. This value corresponds to the average concentration of ^{226}Ra in all tailings piles of 669 pCi/g (DOE, 1990). It is calculated from the third term on the left side of Eq. (1), assuming a bulk density of 1.50 g/cm^3, radon emanation coefficient of 0.35, and porosity of 0.43 (DOE, 1995). The uncertainty distribution for the radon emanation rate in the tailings is based on data indicating that the radon emanation coefficient for Monticello acid and Monticell alkaline mill tailings differs by a factor of approximately 2 (Rogers et al., 1984). The standard deviation assigned to the radon source term corresponds to a value that varies by a factor of 2 between the mean minus two standard deviations and the mean plus two standard deviations.

4.3.3 Source-Term Release

The source-term model used in the groundwater-transport simulations was the MEPAS Computed Source Term Release Model (Streile et al., 1996). The source is conceptualized as a constantly-stirred tank reactor in which the contaminant inventory is homogeneously spread throughout the source volume. During each time step, constituent fluxes to each loss route selected by the user are computed, and then mass is subtracted from the available inventory. After each time step, the remaining inventory is again distributed evenly throughout the source area. The model keeps a mass balance for each constituent and stops releasing mass when the constituent inventory has been depleted. This source-term model is used to calculate radium-226 release rates from the mill tailings for both present and future climatic conditions in scenarios 5-8.

The input data required by the model varies with the source media and loss routes selected by the user. In this assessment, the conceptual-site model for the source consisted of “surface” soils contaminated with Ra-226 and leaching to the groundwater as the loss route. The input parameter values are listed in Table 8. Note that several parameters were varied stochastically. The distribution data for these parameters are listed along with prescribed point values that were used when distributions were deemed unnecessary.

Table 8. Parameter values for source-term model.

Parameter	Point Value	Distribution Type	Min.	Max.	Source
Time Step	1 yr	none	N/A	N/A	1
Source Length	N/A	uniform	0.91 m (3 ft)	550 m (1,800 ft)	2
Source Width	N/A	uniform	0.91 m (3 ft)	260 m (850 ft)	2
Source Thickness	12.5 m (41 ft)	none	N/A	N/A	1,2
Bulk Density	1.54 g/cm^3	none	N/A	N/A	1
Total Porosity	0.43	none	N/A	N/A	2
Moisture Content[4]	0.26	none	N/A	N/A	2
Ra-226 K_d	N/A	uniform	50 ml/g	200 ml/g	1
Ra-226 Water Solubility Limit	4.0×10^{-8} mg/L (40 pCi/L)	none	N/A	N/A	1,2
Ra-226 Inventory	2,290 Ci	none	N/A	N/A	1, 2
Ra-226 Half-Life	1,599 yr	none	N/A	N/A	3
Darcy Percolation Rate (present)	N/A	log uniform	3.6×10^{-13} cm/s	3.8×10^{-9} cm/s	see Section 4.4.1
Darcy Percolation Rate (future)	N/A	log uniform	1.1×10^{-11} cm/s	3.4×10^{-7} cm/s	see Section 4.4.1

[1]Assumed or derived; [2]DOE (1995); [3]CRC (1990); [4]moisture content is assumed constant in MEPAS; N/A: Not Applicable

The parameters with uncertainty distributions were selected because their values varied significantly and because the Ra-226 leaching flux out of the source was highly sensitive to these parameters. Brief descriptions for each of the stochastic parameters and how their distribution parameters were derived are provided below.

Source Length and Width—The area of the source is conceptualized as a rectangle having a length and width. Source length is oriented along the predominant groundwater flow direction in the aquifer. Source width is oriented perpendicular to the predominant groundwater flow direction in the aquifer. In the MEPAS model, constituent fluxes are assumed to leave the bottom of the source homogeneously throughout the entire source area. However, in this case, a liner is placed under the entire source area, and leaks in the liner contribute to the actual downward percolation from the source term. For this reason, the source area was varied in an effort to simulate the leak areas and minimize artificial dilution. The source area was varied by independently varying the source length and source width. Although length and width were varied independently, they were correlated by a correlation coefficient of 0.75 to the effective conductivity of the liner. The source length was varied from 550 m (1,800 ft) down to 0.91 m (3 ft) using a uniform distribution. The source width was varied from 260 m (850 ft) down to 0.91 m (3 ft) using a uniform distribution. The maximum values corresponded to the actual dimensions of the repository, and the minimum dimensions corresponded to the assumed minimum dimensions of the effective leak area beneath the repository.

Ra-226 K_d—The partition coefficient, K_d, is a parameter that describes a constituent's tendency to sorb onto soil solids. It is defined as the ratio of a constituent's particulate concentration (g-contaminant/g-soil) to a constituent's dissolved concentration (g-contaminant/ml-water). The higher a constituent's K_d value, the higher the constituent's tendency to sorb onto soil solids. A constituent's K_d affects its availability in soil water and has the effect of retarding its transport

through the groundwater pathway. Site-specific K_d values for Ra-226 were not available; therefore, the Ra-226 K_d was conservatively estimated at 100 ml/g. It should be noted that estimates for sorption-coefficient values in the literature ranged 500 ml/g for sandy soil to 9100 ml/g for clay (Thibault et al., 1990). Because this value is an estimate and can greatly impact Ra-226 transport, it was treated as a stochastic parameter. It was varied with an assumed uniform distribution between 50 and 200 ml/g. The inventory [Ci], repository volume [m^3], bulk density [g/cm^3], and K_d [ml/g] in Table 8 were used to calculate the concentration of Ra-226 [pCi/ml] in the pore water. If this value was less than the solubility in Table 8, it was multiplied by the product of the Darcy percolation rate and cross-sectional area to calculate the rate of release of Ra-226; otherwise, the solubility was used as the maximum concentration in the pore water.

Darcy Percolation Rate (present and future)—The Darcy percolation rate describes the rate at which water is entering the source zone. The percolation values used in this assessment were derived using the HELP computer model as described in Section 4.3.1. Results of the HELP model indicated that under current conditions, the Darcy percolation could range from a high of 3.8×10^{-9} cm/s to a low of 3.55×10^{-13} cm/s with a log-uniform distribution. Under future conditions, the HELP model indicated that the percolation rate could range from a high of 3.39×10^{-7} cm/s to a low of 1.05×10^{-11} cm/s with a log-uniform distribution. These distributions were used by MEPAS to independently simulate present and future climatic source term releases for scenarios 5-8.

4.3.4 Vadose-Zone Transport

The vadose-zone transport model used for scenarios 5-8 was the MEPAS vadose-zone transport model (Whelan et al., 1996). The vadose-zone model employs a semi-analytical solution to the advective-dispersive equation for solute transport. Solute transport is described by one-dimensional advection vertically downward with longitudinal dispersion. The model assumes that the vadose zone has the same areal extent as the source zone above it and has a uniform thickness that is defined by the user. The soil within the vadose zone is assumed to be homogeneous and isotropic; therefore, separate vadose-zone models must be created and connected in series to simulate a soil profile that has more than one distinct layer.

The conceptual site model for the vadose zone in this assessment (scenarios 5-8) consisted of two distinct elements: (1) a double composite-liner system beneath the repository composed of sand, two geomembrane liners, two geosynthetic clay-liners, and a transmissive leachate collection system; and (2) the undisturbed vadose zone between the liner and the water table (see Figure 6 and Figure 7). Because the sand layer (30 cm thick) and the leachate collection region of the composite-liner system are highly transmissive, only the geomembrane and geosynthetic clay-liner materials were modeled. The parameter values and distributions used for the effective composite-liner system are listed in Table 9.

Two parameters were varied stochastically for the composite liner system based on their range and impact on Ra-226 transport. The Ra-226 partitioning coefficient, K_d, and its distribution were described in Section 4.3.3, and the identical distribution is used for the vadose-zone

models. The distribution for effective saturated hydraulic conductivity of the composite-liner system is more complex and described below.

Table 9. Parameter values for double composite-liner system in vadose-zone model.

Parameter	Point Value	Distribution Type	Min.	Max.	Source
Total Porosity	0.50	none	N/A	N/A	1
Field Capacity	0.40	none	N/A	N/A	2
Saturated Hydraulic Conductivity	N/A	log uniform	$1.0x10^{-9}$ cm/sec	$1.0x10^{-4}$ cm/sec	2
Thickness of composite liner	1.5 cm (0.6 in)	none	N/A	N/A	3
Longitudinal Dispersivity[4]	0.015 cm (0.006 inches)	none	N/A	N/A	2 (1% of thickness)
Bulk Density	1.33 g/cm^3	none	N/A	N/A	2 (=(1-total porosity)*2.65)
Ra-226 K_d	N/A	uniform	50 ml/g	200 ml/g	2

[1]Freeze and Cherry (1979); [2]Assumed or derived; [3]DOE (1995); [4]for vadose zone (Burck et al., 1995); N/A: Not Applicable

The saturated hydraulic conductivity describes the maximum rate at which water can flow through a medium. If the rate of water entering the composite liner system from the medium above (i.e., mill tailings in the source-term model) exceeds the conductivity of the effective composite liner, then the water flux is capped at the saturated hydraulic conductivity value of the effective liner. The liner system, as modeled, consisted of two layers of a 0.15-cm thick geomembrane liner above a ~0.6-cm thick geosynthetic clay liner. The intrinsic values for the saturated conductivities of the two materials ($1x10^{-9}$ cm/s for the geosynthetic clay liner and $2x10^{-13}$ cm/s for the geomembrane liner) were assumed based on literature values (DOE, 1995). We assumed that a distribution of defects could occur in both the geomembrane liner (1 cm^2 holes; see Section 4.3.2 for defect distribution) and the geosynthetic clay liner (1 cm^2 "rolls" or creases caused by overlapping the liner sheets). Estimates revealed that with just one defect hole in the geomembrane liner, the geosynthetic clay liner would provide the limiting conductivity. Assuming a distribution of creases in the clay liner led to an effective conductivity distribution for the composite liner system as shown in Table 9. It should be noted that this effective conductivity is used only if the sampled percolation rate in the source-term model (see Table 8) is greater than the effective liner conductivity. In nearly all cases during present climate conditions, the percolation rate is less than the lowest value of the effective conductivity of the liner, so the effective conductivity of the liner is not limiting. However, for future conditions, the percolation rate will exceed the minimum effective conductivity of the liner in about half the sampled realizations.

The effective conductivity of the liner layer was correlated to source length and width by a moderately positive correlation coefficient of 0.75. This was done to reduce the artificial dilution associated with a simulated large source area having only a few defects in the composite liner system through which contaminant could transport. If the sampled effective conductivity of the liner were small, this would indicate few defects and a smaller area through which transport

could occur. On the other hand, if the sampled effective conductivity were large, this would indicate a larger number of defects and a larger area through which transport could occur (see Section 4.3.3 for more details).

Another vadose-zone "layer" was used to represent the undisturbed soil layer beneath the composite liner system. Two different thicknesses were used in the vadose-zone model to represent vadose-zone transport to the two different aquifers: (1) the shallow alluvial aquifer (scenarios 5-6) and (2) the deeper Burro Canyon aquifer (scenarios 7-8). The transport to each aquifer was modeled in separate runs. The input parameter values and distributions used for the undisturbed soil layer in the vadose-zone model are listed below in Table 10.

Table 10. Parameter values for vadose-zone layer for two aquifers.

Parameter	Point Value	Distribution Type	Min.	Max.	Source
Total Porosity	0.41	none	N/A	N/A	1
Field Capacity	0.18	none	N/A	N/A	1
Hydraulic Conductivity	1.0 cm/sec	none	N/A	N/A	2,3
Thickness of Vadose Zone (Shallow Alluvial Aquifer)	4.6 m (15.0 ft)	none	N/A	N/A	4
Longitudinal Dispersivity[5] (Shallow Alluvial Aquifer)	4.6 cm (0.15 ft)	none	N/A	N/A	2 (1% of thickness)
Thickness of Vadose Zone (Deep Burro Canyon Aquifer)	30 m (100 ft)	none	N/A	N/A	2,4
Longitudinal Dispersivity[5] (Deep Burro Canyon Aquifer)	0.3 m (1.0 ft)	none	N/A	N/A	2 (1% of thickness)
Bulk Density	1.5 g/cm^3	none	N/A	N/A	2
Ra-226 K_d	N/A	uniform	50 ml/g	200 ml/g	2

[1]Morrison et al. (1995); [2]Assumed or derived; [3]Freeze and Cherry (1979); [4]DOE (1995); [5]for vadose zone (Buck et al., 1995); N/A: Not Applicable

4.3.5 Saturated-Zone Transport

Groundwater transport for scenarios 5-8 was simulated using the MEPAS saturated-zone transport model (Whelan et al., 1996). The saturated-zone transport model employs a semi-analytical solution to the advective-dispersive equation for solute transport. Solute transport is described by one-dimensional advection in the predominant groundwater flow direction with three-dimensional dispersion (i.e., longitudinal, lateral, and vertical dispersivities). The model assumes that the saturated-zone layer has an unbounded areal extent and has a uniform thickness that is defined by the user. The soil within the saturated zone is assumed to be homogeneous and isotropic. The peak concentration of contaminants in the groundwater can be determined in the saturated-zone transport model by specifying a location for a receptor well. The model will determine the time varying concentrations at this location and SUMMM records the peak concentration and time of peak concentration for each realization of a stochastic simulation.

Two aquifers were modeled separately with the saturated-zone transport model: (1) the shallow alluvial aquifer (scenarios 5-6) and (2) the deep Burro Canyon aquifer (scenarios 7-8). The input

parameter values used for both aquifers are listed in Table 11. Note that several of the parameters were varied stochastically, and several parameters (dispersivity values) were computed during run-time by the sensitivity/uncertainty module SUMMM. The equations are described in the footnotes to the table. Several important parameters are also discussed in more detail below.

Table 11. Parameter values for saturated-zone model.

Parameter	Value	Distribution Type	Min.	Max.	Source
Total Porosity[a]	N/A	uniform	0.35	0.50	1,2
Darcy Velocity	N/A	log uniform	3.0E-07 cm/sec	3.0E-05 cm/sec	3
Thickness of Aquifer (Burro Canyon aquifer)	30 m (100 ft)	none	N/A	N/A	4
Thickness of Aquifer (alluvial aquifer)	1.2 m (4 ft)	none	N/A	N/A	4
Bulk Density	1.5 g/cm^3	none	N/A	N/A	1,4
Longitudinal Travel Distance to Well Intake[b]	N/A	uniform	0.76 m (2.5 ft)	274 m (901 ft)	4
Horizontal Distance off Plume Center Line to Well Intake	0 m	none	N/A	N/A	1
Vertical Distance Below Water Table To Well Intake	0 m	none	N/A	N/A	1
Longitudinal Dispersivity[c]	N/A	uniform	0.076 m (0.25 ft)	27.4 m (90.1 ft)	1
Lateral Dispersivity[d]	N/A	uniform	0.025 m (0.0825 ft)	9.0 m (29.7 ft)	1
Vertical Dispersivity[e]	N/A	uniform	1.9x10^{-4} m (6.3x10^{-4} ft)	0.069 m (0.23 ft)	1
Ra-226 K_d	N/A	uniform	50 ml/g	200 ml/g	1

[a] Effective porosity set equal to total porosity; [b] Travel distance = ((1/2)*source length) + 1; [c] Longitudinal dispersivity = 0.1*travel distance; [d] Lateral dispersivity = 0.033*travel distance; [e] Vertical dispersivity = 0.00025*travel distance (from Buck et al., 1995)

[1]Assumed or derived; [2]Freeze and Cherry (1979); [3]Smith (2001); [4]DOE (1995)

The total porosity describes the total fraction of void spaces in the aquifer. All void spaces in the aquifer are assumed to be filled with water; however, not all of the water is necessarily contributing to the flow. The effective porosity describes the fraction of the voids that contain flowing water. In this assessment, the effective porosity was set equal to the total porosity because site-specific soil characteristics were not known. The effective porosity affects the velocity of the pore water traveling through the aquifer and, subsequently, the rate at which the contaminant is traveling. A uniform distribution was assumed as shown in Table 11. The range was based on literature values for a sandy soil, which closely matched the composition of the alluvium aquifer.

The Darcy velocity of the groundwater describes the volumetric flux of water through the aquifer. The Darcy velocity is converted to pore-water velocity by dividing Darcy velocity by

the effective porosity. The pore-water velocity represents the actual velocity of the groundwater, which is greater than the Darcy velocity due to the reduced area available for flow in the soil pores (the velocity must increase as the cross-sectional area of flow is reduced to maintain conservation of mass). Finally, the solid-water partitioning coefficient, K_d, for Ra-226 assumes the same distribution as those described in the source-term and vadose-zone models.

4.3.6 Human Exposure

Three modules in MEPAS (Strenge and Chamberlain, 1996) were used to evaluate human exposure in this assessment. In the MEPAS system, chronic human health impacts are computed based on contaminant concentrations in the environment. The process of computing the health impacts from environmental concentrations is broken down into three components or modules: the Chronic Exposure module, the Receptor Intake module, and the Human Health Impact module. The Chronic Exposure module receives as its input time-varying contaminant concentrations in the various exposure media (e.g., ground water, surface water, surface soil, and air) and computes time-averaged concentrations for each exposure pathway selected by the user. The time frame for averaging is specified by the user. Exposure pathways available to the user depend on the exposure medium. Some examples of exposure pathways are drinking water, fish ingestion, meat ingestion, milk ingestion, vegetable ingestion, soil dermal contact, and indoor air inhalation. The Receptor Intake module receives time-averaged concentrations by exposure pathway and computes the time-averaged contaminant intakes and doses by exposure pathway. The model requires the user to specify receptor parameters such as body weight, length of exposure, water intake rates, and air inhalation rates. The Human Health Impact module receives the time-averaged intake and doses by exposure pathway and computes time-averaged human-health effects by exposure pathway as selected by the user. Some examples of health effects available to select are hazard quotient, cancer incidence, cancer fatalities, and dose.

Equations and methodologies used in all three modules are typical of those recommended by the EPA and various state agencies. Default values for many of the equation parameters are provided in MEPAS and are also based on EPA and various agency recommendations; however, the user also has the option of editing each input parameter value through the MEPAS user interfaces. While most parameters have default values provided, certain parameters such as duration of exposure, exposure pathways, intake rates, etc. must be input by the user. Selected input parameter values for each of the three modules are listed below in Table 12, Table 13, and Table 14 for scenarios 5-8 of this assessment. None of the parameters were varied stochastically for this assessment.

As noted in Section 4.1, there are two aquifers (shallow alluvium and Burro Canyon) associated with the site. The water usage for each aquifer was assumed to be different as shown in Table 12. It was assumed that the shallow alluvial aquifer was used for agricultural purposes only and that the deeper Burrow Canyon aquifer was used for both agricultural purposes and drinking water.

Table 12. Parameter values for chronic exposure module.

Parameter	Value
Time to start exposure computation (alluvial aquifer)[1]	10,000 years
End time for exposure computation (alluvial aquifer)[1]	20,000 years
Number of evaluation points (alluvial aquifer)[2]	334
Time to start exposure computation (Burro Canyon aquifer)[1]	12,000 years
End time for exposure computation (Burro Canyon aquifer)[1]	27,000 years
Number of evaluation points (Burro Canyon aquifer)[2]	500
Exposure duration	30.0 years
Exposure pathways selected (alluvial aquifer)	leafy vegetable ingestion, other vegetable ingestion, meat ingestion, milk ingestion
Agricultural water usage (alluvial aquifer)	crop irrigation, animal drinking, and irrigation of animal feed
Fraction of the year that groundwater is used for irrigation (alluvial aquifer)	1.0
Irrigation rate (alluvial aquifer)[3]	100 L/m^2/month
Exposure pathways selected (Burro Canyon aquifer)	drinking water, leafy vegetable ingestion, other vegetable ingestion, meat ingestion, milk ingestion
Agricultural water usage (Burro Canyon aquifer)	crop irrigation, animal drinking, and irrigation of animal feed
Fraction of the year that groundwater is used for irrigation (Burro Canyon aquifer)	1.0
Irrigation rate (Burro Canyon aquifer)	100 L/m^2/month

[1]The start and end times for the exposure computation are estimated based on the calculated times for peak concentration in the saturated-zone transport model

[2]The number of evaluation points was chosen to yield an exposure duration of 30 years.

[3]Default value in MEPAS (Strenge and Chamberlin, 1995)

Table 13. Parameter values for receptor intake module.

Parameter	Value[1]
Body weight of individual	70 kg
Exposure duration	30.0 yr
Ingestion rate of leafy vegetables	0.021 kg/d
Ingestion rate of other vegetables	0.13 kg/d
Ingestion rate of meat	0.065 kg/d
Ingestion rate of milk	0.075 L/d
Ingestion rate of water	2 L/d

[1]Default values used in MEPAS (Strenge and Chamberlin, 1995)

Table 14. Parameter values for human health impact module.

Parameter	Value
Health metric	radiation dose commitment

4.4 Results and Discussion

The results of the stochastic simulations are presented in the following sections for scenarios 1-8 (see Table 3). The results of scenarios 1 and 2 (water percolation through the cover) are presented in Section 4.4.1; the results of scenarios 3 and 4 (radon gas transport through the cover) are presented in Section 4.4.2; the results of scenarios 5 and 6 (radium transport to the shallow alluvial aquifer) are presented in Section 4.4.3; and the results of scenarios 7 and 8 (radium transport to the deep Burro Canyon aquifer) are presented in Section 4.4.4.

4.4.1 Percolation through the Cover

As discussed in Section 4.3.1, the code HELP was used to simulate the range of percolation fluxes through the cover at Monticello. Results of the Monte Carlo simulations using the HELP code are presented as a cumulative probability in Figure 9 for both present-day (scenario 1) and future conditions (scenario 2). The simulations for future conditions included additional uncertainty in input parameters such as precipitation, temperature, and integrity of the geomembrane liner. Results show that the uncertainty in the input parameters cause a large range in the percolation through the cover (5-6 orders of magnitude). The performance of the cover under future conditions is seen to be worse (higher percolation through the cover) because of the potential for increased precipitation and a degraded geomembrane liner. However, the cumulative distributions for both present-day and future conditions are generally below the maximum hydraulic conductivity value of $1x10^{-7}$ cm/s as prescribed in 40 CFR 264.301. The probabilistic results shown in Figure 9 indicate that there is no risk under present-day conditions that the percolation through the cover will exceed the regulatory requirement for maximum hydraulic conductivity, but this probability increases to approximately 5% for future conditions (we assume a unit gradient, making the percolation flux and hydraulic conductivity equivalent).

An important feature of the probabilistic calculations is that sensitivity analyses can be performed to determine which parameters are most important to the simulated performance metric (e.g., water percolation). A stepwise linear-regression was performed between the rank-transformed input parameters and the water percolation reaching the mill tailings. Results of the stepwise regression are summarized in Table 15. The most important parameters for both present and future conditions are the placement quality of the geomembrane liner (see Schroeder et al., 1994a,b for details), the saturated hydraulic conductivity of the topsoil layer, and the wilting point of the clay layer. These findings are important because they can be used to prioritize parameters for additional data collection or long-term monitoring.

Table 15. Summary of parameters important to simulated water percolation through the cover based on stepwise linear-regression analysis.

Step	Variable	R^2	ΔR^2
Present Climate			
1	placement quality	0.4382	0.4382
2	Ksat-layer 1	0.6132	0.1750

Step	Variable	R^2	ΔR^2
3	wilting point – layer 4	0.6600	0.0468
4	wilting point – layer 2	0.6733	0.0133
5	evaporative zone depth	0.6824	0.0091
Future Climate			
1	placement quality	0.4513	0.4513
2	Ksat – layer 1	0.6096	0.1583
3	wilting point – layer 4	0.7213	0.1117
4	precipitation multiplier	0.7869	0.0656
5	temperature adjustment	0.7957	0.0088
6	maximum leaf-area index	0.8044	0.0087

Alternative cover designs were also evaluated for the Monticello disposal site using probabilistic calculations. The performance of an evapotranspiration (ET) cover (Dwyer, 2000) was evaluated using the same probabilistic methods described for the existing design. The ET cover consists of only the top layer shown in Figure 5. Results of the probabilistic assessment of the ET cover are shown in Figure 10. Although the ET cover does not perform as well as the existing design, the majority of the realizations yield percolation fluxes that are less than the regulatory limit. In addition, the ET cover is much cheaper to construct than similar designs such as the one at Monticello (Dwyer, 2000). An assessment of cost vs. performance can be made based on these results. This example illustrates the use of probabilistic simulations and risk-based performance metrics to evaluate alternative designs for long-term covers.

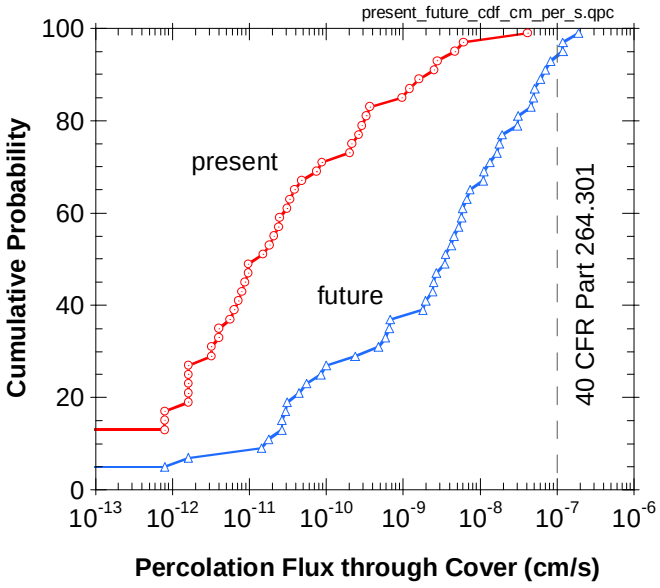

Figure 9. Cumulative probability distribution of water percolation reaching the mill tailings for present and future conditions (scenarios 1 and 2).

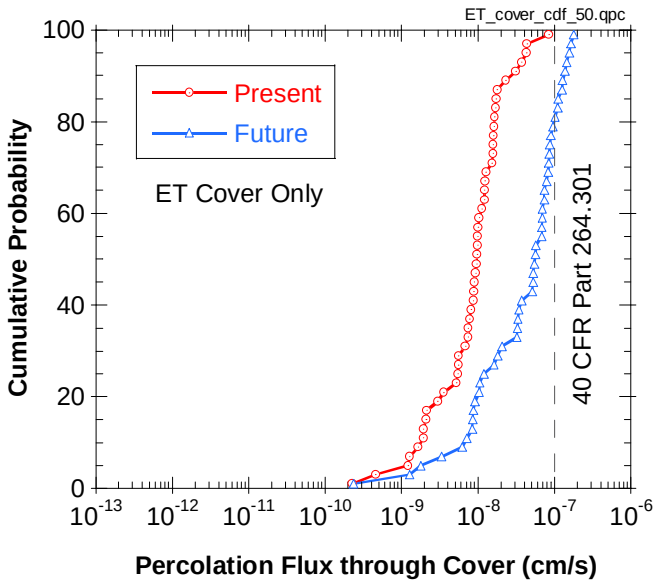

Figure 10. Cumulative probability distribution of water percolation reaching the mill tailings for present and future conditions for an alternative ET cover design.

4.4.2 Radon Gas Flux at the Surface

Probabilistic analyses of radon gas transport for the landfill cover performance assessment were performed using the FRAMES computer program. The RAECOM computer code was coupled into the FRAMES code as an alternative model in the source module. The RAECOM model in the source module was linked to the sensitivity module in FRAMES and 100 realizations of the system were simulated for present conditions and for future conditions (scenarios 3-4).

The results of these simulations are shown in Figure 11. For present climatic conditions and essentially undegraded geomembrane performance, the simulated Rn-222 flux at the land surface spans approximately three orders of magnitude with a maximum value of about 1 pCi/m^2-s. The median value among the 100 realizations of cover performance is about 0.16 pCi/m^2-s for present conditions. For future conditions (>100 years), the simulated Rn-222 flux at the land surface spans approximately three orders of magnitude with a maximum value of about 29 pCi/m^2-s. It should be noted that the uncertainty reflected in the results for future conditions is significantly broader than the uncertainty for present conditions in absolute (linear) terms. The median value among the 100 realizations of cover performance is about 3.4 pCi/m^2-s for future conditions.

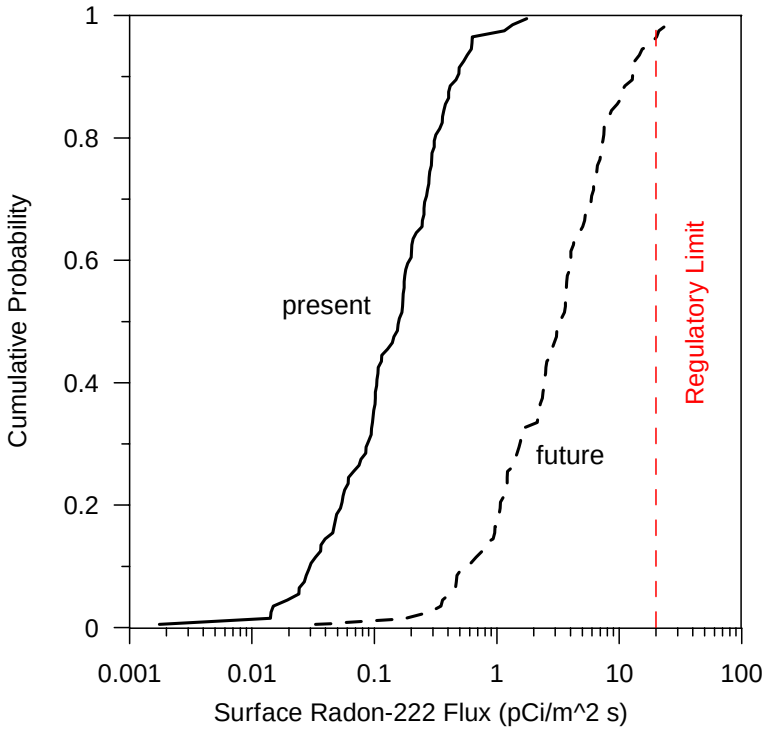

Figure 11. Cumulative probability distribution of simulated radon flux at the land surface for present and future conditions (scenarios 3 and 4).

Most of the variability among realizations for both the present and future conditions is attributable to uncertainty in the values of the effective diffusion coefficient in the tailings and cover layers. Uncertainty in the radon source term and the values of moisture content contribute to overall uncertainty in the system performance to a lesser extent.

The difference between the results for present conditions and future conditions is due primarily to potentially degraded performance of the geomembrane as a diffusion barrier in the future. Uncertainty exists with regard to the impact of numerous degradation processes for high-density polyethylene geomembranes and estimates suggest a lifetime of several hundred years (Koerner et al., 1991; Hsuan and Koerner, 1998). It should be noted that in the model the geomembrane layer functions as a significant barrier to diffusion only at relatively low values of defect density, primarily due to the relative thinness of the layer. In addition, the somewhat higher values of moisture content in the tailings for future, wetter climatic conditions lead to enhanced radon diffusion due to the reduced volume of the air phase in the medium.

The results for both the present and future conditions are influenced by a competing interaction between two parameters in the model for radon transport. Transport of radon gas by diffusion is enhanced at higher moisture content because of the reduced air-phase volume in the soil under these conditions. This enhancement is due to the relatively higher radon concentration in the air phase (same radon mass in a smaller volume of air) and the resulting larger concentration gradient between the mill tailings and the atmosphere at land surface. In a competing manner,

higher moisture content results in a lower effective diffusion coefficient for radon gas. This relationship is represented by the negative correlation between moisture content and effective diffusion coefficient in this study. The aggregate impact of this competing interaction between moisture content and effective diffusion coefficient on the probabilistic analyses conducted for this study is not clear, but is probably dominated by variability in the diffusion coefficient.

Overall, these results indicate a high degree of confidence (nearly 100%) that the landfill cover design at Monticello meets the performance objective of 20 pCi/m^2-s of Rn-222 flux from the tailings at the land surface for present conditions. The simulation results for future conditions indicate relatively high confidence (approximately 97%) that the Rn-222 flux from the tailings at the land surface will be less than the regulatory limit. The expected performance of the landfill cover design for future conditions, as represented by the median (3.4 pCi/m^2-s) or the mean (5.0 pCi/m^2-s) is significantly lower than the regulatory limit.

It should be noted, however, that the analyses of radon gas transport for this study are based on nominal behavior of the landfill cover system. The thickness of each layer in the design is fixed in this performance assessment. Consequently, these analyses do not address scenarios that could impact the thickness of the cover (e.g., erosion or subsidence). In addition, some processes and features that could potentially compromise performance of the cover system as a diffusion barrier (e.g., animal burrowing and desication cracking) were not explicitly evaluated.

4.4.3 Groundwater Concentration and Exposure Assessment for the Shallow Alluvial Aquifer

In this section (and the next), two performance metrics were recorded during the FRAMES groundwater transport simulations: 1) the peak Ra-226 concentration in the water crossing the down-gradient boundary of the repository and 2) the peak total dose for Ra-226 and its progeny for specified exposure pathways associated with the consumption of groundwater from a well at the down-gradient boundary of the waste site.

The peak groundwater concentrations for Ra-226 [pCi/L] were recorded in FRAMES for 100 realizations of pore-water transport from the mill tailings to the shallow alluvial aquifer (scenarios 5-6). Cumulative probabilities of the peak concentration are plotted in Figure 12 for both present and future conditions. These results can be used to determine the probability of exceeding the maximum contaminant level (MCL) or risk-based concentration; the MCL for Ra-226 is 5 pCi/L (40 CFR 192.02(a) and 40 CFR 192(b)(2)).

Results indicate that the simulated maximum Ra-226 concentration in the groundwater is approximately 0.2 pCi/L, which is less than the MCL. The low peak concentrations are attributable mainly to the low percolation rates through the source, high K_d values for Ra-226, and a relatively short half-life for Ra-226. The percolation rate range computed by the HELP model for current conditions was 3.55E-13 cm/s to 3.80E-09 cm/s. The percolation rate computed by the HELP model for future conditions was 1.05E-11 cm/s to 3.39E-07 cm/s. These low percolation rates coupled with high K_d values that ranged from 50 ml/g to 200 ml/g resulted in long travel times to the receptor well. In all modeling runs, the times of peak concentrations were between 7,000 and 15,000 years. These long travel times coupled with a half-life for Ra-

226 of 1,599 years resulted in the low peak concentrations at the receptor well location. Therefore, the stochastic modeling in this assessment indicates that for both current and future conditions there is no risk of exceeding the MCL. However, it should be emphasized that a number of assumptions (albeit conservative) were made in the development of this model, and only a limited number of features, events, and processes were considered.

Figure 12 also shows that the concentrations for future conditions are greater than the concentrations for present conditions by 2-3 orders of magnitude . The primary reason is the increased infiltration rate during future conditions caused by greater precipitation and more degradation of the cover and liner materials. It should also be noted that the simulations for both present and future conditions result in a large range of concentrations due to the large range of stochastic parameter distributions that were used in the models. Future simulations will attempt to provide a sensitivity analysis and reduce the uncertainty in these parameters with more refined data.

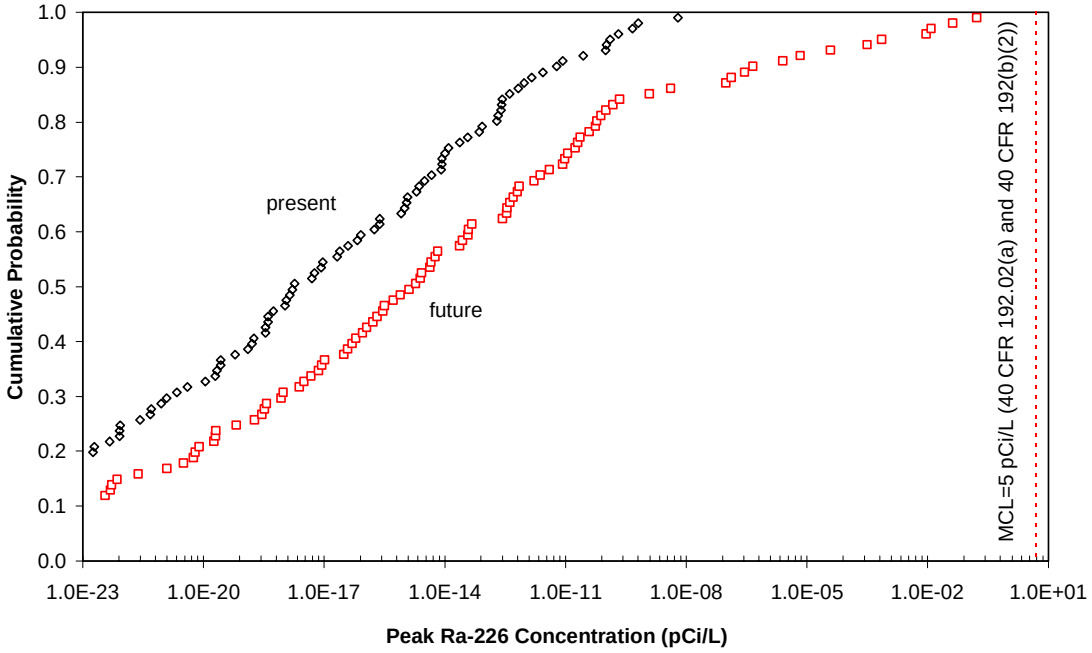

Figure 12. Cumulative probability distribution for peak Ra-226 concentration in the shallow alluvial aquifer for present and future conditions (scenarios 5-6). Note: concentration values of 0 are not plotted on the log scale.

The cumulative probability distribution for dose (millirem per year) resulting from the shallow alluvial aquifer simulations were plotted for both present and future conditions. In MEPAS, the cumulative dose was recorded over a moving 30-year period, and the dose rate in millirem per year was calculated by dividing the peak cumulative dose by 30 years. The maximum effective

dose equivalent for all radionuclides and all routine DOE exposure pathways is 100 mrem/year (DOE Order 5400.5 II 1.a).

For both the current and future conditions, the peak cumulative dose from Ra-226 and its decay products for all pathways is 0.78 mrem/year, which is considerably less than the maximum effective dose equivalent. However, only Ra-226 and its progeny were considered in this assessment, and only the groundwater pathway was evaluated. In addition, the low peak cumulative doses are attributable to the low percolation rates through the source, high K_d values for Ra-226, and a relatively short half-life for Ra-226. In all modeling runs, the times of peak cumulative doses were between 10,000 and 17,000 years. These long travel times coupled with a half-life for Ra-226 of 1,599 years resulted in the low peak cumulative doses for the exposures associated with water usage from the receptor well location. Also it should be noted that the time of peak cumulative dose may vary from the time of peak Ra-226 concentration at the groundwater well. The cumulative dose incorporates the doses due to progeny as well, and progeny may peak at different times than the parent constituent (different half-lives and different K_d values; the K_d values for the progeny were assumed to be1000 ml/g).

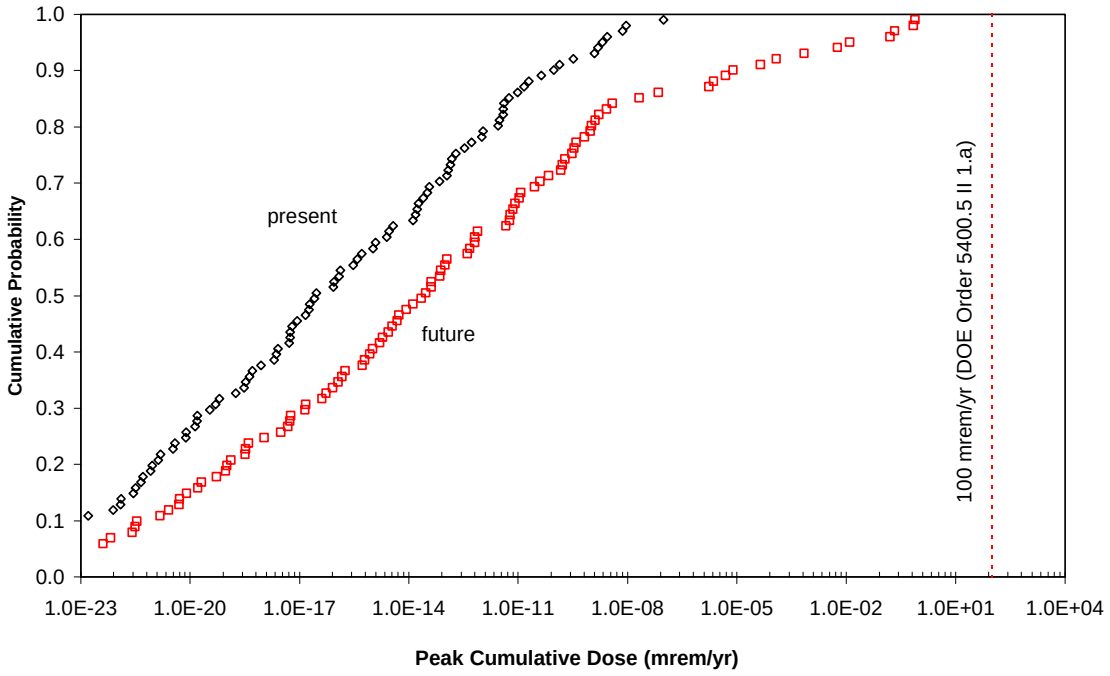

Figure 13. Cumulative probability distribution for peak cumulative dose for Ra-226 and its progeny from the shallow alluvial aquifer for present and future conditions (scenarios 5-6). Note: dose values of 0 are not plotted on the log scale.

Similar to the cumulative distribution for concentration, the dose results in Figure 13 show that there is a large spread in the results. In addition, the future conditions yield doses that are 2-3

orders of magnitude larger than the doses for present-day conditions. Future analyses will consider sensitivity analyses and the reduction of uncertainty in the input parameters.

4.4.4 Groundwater Concentration and Exposure Assessment for the Burro Canyon Aquifer

The results presented in this section are similar to the results presented in the preceding section. The only difference in the conceptual models is that the groundwater concentration and exposure assessment are performed for the deeper Burro Canyon aquifer (scenarios 7 and 8) as opposed to the shallow alluvial aquifer (scenarios 5 and 6).

Simulations of Ra-226 transport from the mill tailings to the Burro Canyon aquifer resulted in undetectable (zero) concentrations in the groundwater during the simulation period for nearly all conditions. The simulations with present climatic conditions resulted in zero groundwater concentrations for all realizations in the Burro Canyon aquifer. The value for the peak Ra-226 concentration in the groundwater under future conditions was $5x10^{-11}$ pCi/L, which is well below the MCL of 5 pCi/L. The extremely low (or zero) concentrations are due to the low percolation rates through the source, high K_d values for Ra-226, and a relatively short half-life for Ra-226 that resulted in long travel times to the receptor well in the aquifer (the two non-zero concentrations simulated under future conditions occurred at 8,000 and 14,000 years). The concentrations predicted for the Burro Canyon aquifer are significantly lower than those for the shallow alluvial aquifer due to the difference in thickness of the vadose zones. The vadose-zone depth to the alluvial aquifer is 4.6 m (15 ft), while the vadose-zone depth to the Burro Canyon aquifer is 30 m (100 ft). The added depth leads to longer travel times and greater decay of Ra-226.

Figure 14 shows the simulated cumulative distribution for peak dose resulting from transport of Ra-226 to the Burro Canyon aquifer. Only the results for the future infiltration scenario are presented in the figure because the results for the present conditions resulted in doses that were zero for all realizations. The models simulating future conditions resulted in a peak cumulative dose of $8.62x10^{-10}$ mrem/year, which is well below the regulatory limit. The peak cumulative doses occurred between 12,000 and 18,000 years in all the simulations, which are longer than the times of peak doses for the shallow alluvial aquifer. The doses predicted for the Burro Canyon aquifer are significantly lower than those for the alluvial aquifer due to the difference in thickness of the vadose zones. The added depth leads to longer travel times and thus more time for the Ra-226 to decay. Also it should be noted that the time of peak cumulative dose may vary from the time of peak Ra-226 concentration at the groundwater well. The cumulative dose incorporates the doses due to progeny, and progeny may peak at different times than the parent constituent.

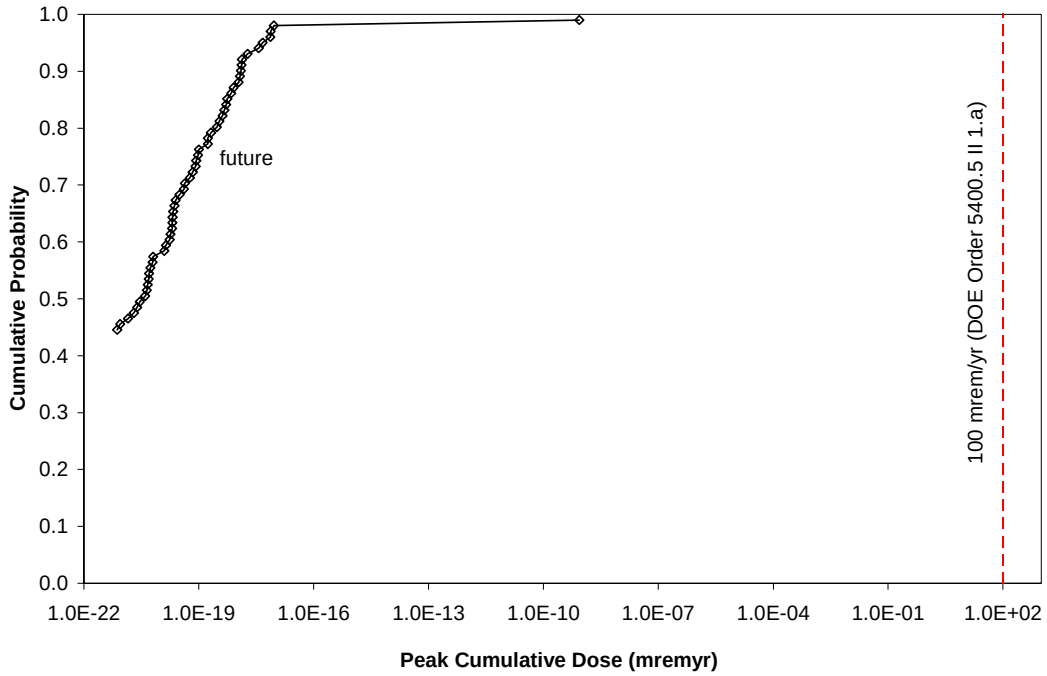

Figure 14. Cumulative probability distribution for peak cumulative dose for Ra-226 and its progeny from the Burro Canyon aquifer for future conditions (scenario 8). Note: dose values of 0 are not plotted on the log scale.

5. Summary and Conclusions

This report has presented a method for conducting performance-assessment analyses for long-term cover systems. The systematic approach consists of five basic steps:

1. Develop and screen scenarios based on regulatory requirements (performance objectives) and relevant features, events, and processes
2. Develop models of relevant features, events, and processes
3. Develop values and/or uncertainty distributions for input parameters
4. Perform calculations and sensitivity/uncertainty analyses
5. Document results and provide feedback to previous steps and associated areas to improve calculations as needed

This method was illustrated with a performance assessment of the uranium mill-tailings repository at Monticello, Utah. A number of scenarios were considered in the assessment that

evaluated several key performance metrics: (1) water percolation through the cover; (2) radon gas transport through the cover; (3) concentration of radium-226 in the groundwater; and (4) human exposure to radium-226. A summary of the scenarios considered and their respective performance objectives are summarized in Table 3. Representative features, events, and processes (FEPs) were identified for each scenario, but not all FEPs (e.g., human intrusion) were considered in this assessment.

The software FRAMES was used to integrate various components into a total-system model. FRAMES employs a drag-and-drop icon-based architecture that allows models of different processes and different media to be linked to one another. Component models that were used in FRAMES included several MEPAS modules: source-term model, vadose-zone transport model, saturated-zone transport model, and human-exposure models. In addition, a radon-gas transport code, RAECOM, was integrated into FRAMES as part of this study. The code HELP was used independently of FRAMES to determine the amount of water that could percolate through the cover to the waste. In each model, and in the total-system model, uncertainty analyses were performed using distributions of stochastic parameters that were determined to have a large range and/or a significant impact on the simulated performance metric. Values and ranges for input parameter distributions were obtained using existing data, literature, and professional judgment.

Monte Carlo simulations were performed to obtain a distribution of results that could be compared to the desired performance objective for each scenario. Present and future climatic conditions were considered independently in the scenarios. For future conditions, additional uncertainty was added to parameters such as precipitation and geomembrane degradation in the cover. In nearly all the simulations, the simulated results were well below the desired performance objectives for both present and future conditions.

The model of water percolation through the cover resulted in just a few realizations (all during future climatic conditions) that produced percolation fluxes exceeding 10^{-7} cm/s. A curve fit was applied to the results to create a log-normal distribution of percolation fluxes that was used in the source-term model in FRAMES. In addition, a stepwise linear regression revealed that the most important parameters for water percolation through the cover were geomembrane placement quality, hydraulic conductivity of the topsoil layer, and wilting point of the clay layer. Finally, an alternative ET cover design was also evaluated and compared to the performance objectives. Although the ET cover did not perform as well as the existing Monticello cover, the results indicated that the simulated percolation fluxes through the ET cover had a very low risk of exceeding the performance objective. This scenario helped to illustrate the usefulness of probabilistic analyses to compare alternative designs for long-term covers. In addition, these results showed how important parameters could be identified with sensitivity analyses for use in prioritizing additional data collection and long-term monitoring studies.

The radon-gas transport analysis revealed that nearly all of the realizations yielded surface Ra-222 fluxes that were below the regulatory limit of 20 pCi/m^2-s. Important parameters in this model were the effective diffusion coefficient and moisture content in the different layers of the cover. The moisture content was found to have an interesting impact on the diffusive flux of radon gas from the mill tailings to the surface of the cover. An increase in moisture content decreased the effective diffusion coefficient due to the reduced area for diffusion. However, an

increased moisture content also increased the concentration gradient through the cover by reducing the available pore space for radon gas to occupy.

Transport of radium-226 from the mill tailings to two different aquifers was also evaluated under present and future conditions. Transport to both a shallow alluvial aquifer and a deeper regional (Burro Canyon) aquifer was simulated independently. Groundwater concentrations and dose to a human were used as the performance metrics in these simulations. In all simulations, the simulated groundwater concentration and dose were less than the desired performance objectives (5 pCi/L and 100 mrem/yr). Important parameters for these simulations included the low percolation fluxes (from the model of water percolation through the cover) and the relatively large sorption coefficients for radium-226 in both the vadose and saturated zones.

Overall the results of this performance assessment illustrated how probabilistic analyses could be used to evaluate long-term performance of covers against regulatory metrics. The performance metrics can be risk-based, such as groundwater concentration or dose, or they can be prescriptive metrics such as conductivity for a particular layer of the cover. In both cases, probabilistic performance assessments can provide uncertainty and sensitivity analyses that identify the parameters that are most important to long-term performance. These parameters may be important for engineering design, environmental studies, and long-term monitoring efforts to assist in prioritizing their efforts. In addition, alternative designs for long-term covers can be evaluated using risk-based performance metrics that are intended to protect human health and the environment. These comparisons provide a more quantitative means to compare the performance of cover designs while factoring in additional issues such as cost and schedule.

Long-lived contaminants will remain in the Monticello landfill and many other closure sites being managed by DOE. To address the long-term management of these closure sites, the DOE has created a “stewardship” program. This DOE stewardship program encompasses the activities required to maintain an adequate level of protection of human health and the environment posed by wastes and residual contamination after cleanup is complete (DOE, 1999).

DOE’s commitment to provide long-term environmental stewardship may require DOE to consider performance objectives more stringent that those set by applicable regulations. As an example, a regulation may require that performance be assessed for 30 years, even when addressing long-lived contaminants. From a risk-based perspective, DOE is best served by considering features, events, and processes at the site that may contribute to the long-term risk of groundwater contamination and human exposure. Analysis of performance over long time periods provides the opportunity to examine the impacts of a range of geologic conditions on the ability of the engineered and natural barriers to limit releases to the biosphere. Therefore it may be in DOE’s best interest to consider the long-term performance of a closure system, even if the regulations only address the near-term performance.

6. References

Abraham, J.D. and W.J. Waugh, 1995, Cover drainage and leakage rate estimation using the help 3.1 code, Calc. No. E0267102, Rust Geotech Inc., Grand Junction, CO.

Buck, J. W., G. Whelan, J. G. Droppo, Jr., D. L. Strenge, K. J. Castleton, J. P. McDonald, C. Sato, and G. P. Streile, 1995, Multimedia environmental pollutant assessment system (MEPAS): application guidance -- guidelines for evaluating MEPAS input parameters for version 3.1, PNL-10395, Pacific Northwest Laboratory, Richland, Washington.

Carsel, R.F. and R.S. Parrish, 1988, Developing joint probability distributions of soil water retention characteristics, Water Resources Research, vol. 24, no. 5, pp. 755-769.

Cranwell, R.M., R.V. Guzowski, J.E. Campbell, and N.R. Ortiz, 1982, Risk methodology for geologic disposal of radioactive waste: scenario selection procedure, NUREG/CR-1667 (SAND80-1429), U.S. Nuclear Regulatory Commission, Washington DC.

CRC (Chemical Rubber Company), 1990, Handbook of chemistry and physics, 71st ed., CRC Press, Boca Raton, FL.

Daniel B. Stephens and Associates, Inc., 1993, Laboratory analysis of soil hydraulic properties of Monticello remedial action project samples, Albuquerque, New Mexico.

DOE (U.S. Department of Energy), 1990, Final remedial investigation/feasibility study—environmental assessment for the Monticello, Utah, Uranium Mill Tailings Site, DOE/ID/12584-21, U.S. Department of Energy, Washington, D.C.

DOE, 1995, Monticello remedial action project operable unit i millsite remediation pre-final design, MR-E-95-04, Engineering Document Number E01425AD, U.S. Department of Energy, Washington, D.C.

DOE, 1996, Title 40 CFR 191 compliance certification application for the Waste Isolation Pilot Plant, 21 vols. DOE/CAO-1996-2184. U.S. Department of Energy, Carlsbad Area Office, Carlsbad, NM.

DOE, 1998, Viability assessment of a repository at Yucca Mountain. DOW/RW-0508. U.S. Department of Energy, Office of Civilian Radioactive Waste Management, Washington, D.C.

DOE/EM-0362, 1998, Accelerating Cleanup: paths to closure, June 1998.

DOE, 1999, From Cleanup to stewardship, Appendix. D, DOE/EM-0466.

DOE Order 5400.5, 1993, Radiation Protection of the Public and the Environment.

DOE M 435.1-1, 1999, Radioactive waste management manual, p. IV-11, approved 7/9/99.

Dwyer, S. F., B. R. Reavis, and G. Newman, 2000, Alternative landfill cover demonstration, FY2000 annual data report, SAND2000-2427, Sandia National Laboratories, Albuquerque, New Mexico.

EPA (U.S. Environmental Protection Agency), 40 CFR 61, National Emissions standards for hazardous air pollutants

EPA, 40 CFR 141, National primary drinking water regulations.

EPA, 40 CFR 192, Health and Environmental protection standards for uranium and thorium mill tailings

Fayer, M.J., 2000, UNSAT-H Version 3.0: Unsaturated Soil Water and Heat Flow Model - Theory, User Manual, and Examples," PNNL-13249, Pacific Northwest National Laboratory, Richland, WA.

Fleenor, W.E., and I.P. King, 1995, Identifying limitations on use of the help model, Landfill Closures - Environmental Protection and Land Resources, Geotechnical Special Publication No. 53, Dunn and Singh, eds., ASCE.

Freeze, R.A., and J.A. Cherry, 1979, Groundwater, Prentice-Hall Inc.,Englewood Cliffs, N.J.

Ho, C.K. and S.W. Webb, 1998, Capillary Barrier performance in heterogeneous porous media, Water Resources Research, Vol. 34, No. 4, pp. 603-609.

Hsuan, Y.G. and R.M. Koerner, 1998, Antioxidant depletion lifetime in high density polyethylene geomembranes, Journal of Geotechnical and Geoenvironmental Engineering, vol. 124, no. 6, pp. 532-541.

Koerner, R.M., Y. Halse-Hsuan, and A.E. Lord, 1991, Long-term durability of geomembranes, Civil Engineering, April, 1991, pp. 56-58.

MACTEC, 2000, Monticello Mill Tailings Site Operable unit III, Interim remedial action progress report, Prepared for the DOE, Grand Junction Office, Machtech ER, Grand Junction Colorado, Q00197AA.

Meyer, P. D. and G. W. Gee, 1999, Information on hydrologic conceptual models, parameters, uncertainty analysis, and data sources for dose assessments at decommissioning sites, NUREG/CR-6656, U.S. Nuclear Regulatory Commission, Washington, D.C.

Meyer, P. D. and R. Y. Taira., 2001, Hydrologic uncertainty assessment for decomissioning sites: hypothetical test case applications, NUREG/CR-6695, U.S. Nuclear Regulatory Commission, Washington, D.C.

Morrison, S.J., V.S. Tripathi, and R.R. Spangler, 1995, Coupled reaction/transport modeling of a chemical barrier for controlling uranium(VI) contamination in groundwater, Journal of Contaminant Hydrology, vol. 17, pp. 347-363.

NRC (U.S. Nuclear Regulatory Commission), 1989, Calculation of Radon flux attenuation by earthen uranium mill tailings covers, Regulatory Guide 3.64, U.S. Nuclear Regulatory Commission, Washington, D.C.

Owenby, J. R. and D. S. Ezell, 1992, Monthly station normals of temperature, precipitation, and heating and cooling degree days 1961-90 Utah, National Oceanic and Atmospheric Administration, U.S. Department of Commerce, Asheville, NC.

Pruess, K., 1991, TOUGH2—A general-purpose numerical simulator for multiphase fluid and heat flow, *LBL-29400*, Lawrence Berkeley Laboratory, Berkeley, CA.

Rogers, V.C., K.K. Nielson, and D.R. Kalkwarf, 1984, Radon attenuation handbook for uranium mill tailings cover design, NUREG/CR-3533, U.S. Nuclear Regulatory Commission, Washington, D.C.

Schroeder, P. R., Aziz, N. M., Lloyd, C. M. and Zappi, P. A., 1994a, The hydrologic evaluation of landfill performance (HELP) model: User's Guide for Version 3, EPA/600/R-94/168a, September 1994, U.S. Environmental Protection Agency Office of Research and Development, Washington, DC.

Schroeder, P. R., Dozier, T.S., Zappi, P. A., McEnroe, B. M., Sjostrom, J. W., and Peyton, R. L., 1994b, The hydrologic evaluation of landfill performance (HELP) model: engineering documentation for version 3, EPA/600/R-94/168b, September 1994, U.S. Environmental Protection Agency Office of Research and Development, Washington, DC.

Smith, G., 2001, personal communication in e-mail dated 5/23/2001.

Streile, G.P., Shields K.D., Stroh J.L., Bagaasen L.M., Whelan G., McDonald J.P., Droppo J.G., and Buck J.W., 1996, The multimedia environmental pollutant assessment system (MEPAS): source-term release formulations. PNNL-11248, Pacific Northwest National Laboratory, Richland, WA..

Strenge, D.L. and P.J. Chamberlin, 1995, Multimedia environmental pollutant assessment system (MEPAS): exposure pathway and human health impact assessment models. PNNL-10523, Pacific Northwest National Laboratory, Richland, WA..

Thibault, D.H., M.I. Sheppard, and P.A. Smith, 1990, A critical compilation and review of default soil solid/liquid partition coefficients, Kd, for use in environmental assessments, AECL-10125, Atomic Energy of Canada Limited Research Company.

van Genuchten, M. Th., F. J. Leij, and S. R. Yates, 1991, The RETC code for quantifying the hydraulic functions of unsaturated soils, Version 1.0. EPA Report 600/2-91/065, U.S. Salinity Laboratory, USDA, ARS, Riverside, California.

Waugh, W.J., 2001, personal communication in e-mail dated 2/20/2001.

Waugh, W. J. and K. L. Petersen, 1994, Paleoclimatic data application: long-term performance of uranium mill tailings repositories, in Proceedings of "Climate Change in the Four Corners and Adjacent Regions: Implications for Environmental Restoration and Land-Use Planning," CONF-9409325, Grand Junction, CO, September 12-14, 1994.

Whelan, G, J.W. Buck, D.L. Strenge, J.G. Droppo, B.L. Hoopes, R.J. Aiken, 1992, Overview of the multimedia environmental-pollutant assessment system (MEPAS), Hazardous Waste & Hazardous Materials, 9(2), pp. 191-208.

Whelan G, McDonald JP, and Sato C., 1996, The multimedia environmental pollutant assessment system (MEPAS): groundwater pathway formulations. PNNL-10907, Pacific Northwest National Laboratory, Richland, WA.

Wyss, G.D. and K.H. Jorgensen, 1998, A user's guide to LHS: Sandia's Latin Hypercube Sampling Software, SAND98-0210, Sandia National Laboratories, Albuquerque, NM.

Appendix A: Parameter Values and Distributions for Material Properties of the Monticello Cover

This Appendix details the base-case parameters and the derivation of uncertainty distributions for various layers in the Monticello cover. The base-case parameters used in the HELP calculations are shown in Tables A-1 and A-2:

Table A-1. Base-Case Input Parameters for Cover Layers

Input Parameter		Value	Source
Layer 1 Vertical Percolation Layer	Thickness (in)	66.0	(1)
	Porosity	0.456	(1)
	Field Capacity	0.380	(1)
	Wilting Point	0.180	(1)
	Initial Water Content	0.300	(1)
	K_{sat} (cm/sec)	10^{-4}	see Section 4.3.1
Layer 2 Lateral Drainage Layer	Thickness	12.0	(1)
	Porosity	0.375	(1)
	Field Capacity	0.150	(1)
	Wilting Point	0.040	(1)
	Initial Soil Water Content	0.080	(1)
	K_{sat} (cm/sec)	10^{-2}	(1)
	Slope (%)	3	(1)
	Drainage Length (ft)	1800.	(1)
Layer 3 Flexible membrane Liner	Thickness (in)	0.060	(1)
	K_{sat} (cm/sec)	2.0×10^{-13}	(1)
	Pinhole Density (Holes/Acre)	1.0	(1)
	Installation defects (holes/acre)	1.0	(1)
	Placement Quality	"Good"	(1)
Layer 4 Radon Barrier	Thickness (in)	24.0	(1)
	Porosity	0.343	(1)
	Field Capacity	0.200	(1)
	Wilting Point	0.150	(1)
	Initial Soil Water Content	0.310	(1)
	K_{sat} (cm/sec)	10^{-7}	(1)

(1) Abraham and Waugh (1995)

Table A-2. HELP Base-Case General Input Parameters

Input Parameter		Value	Source
Cover Slope (%)		3.0	(1)
Cover Length (ft)		1800.	(1)
SCS Runoff Curve Number		92	(1)
Evaporative Zone Depth (in)*		66.0	(1)
Maximum Leaf-Area Index*		1.0	(1)
Growing Season	Start - DOY*	74	(1)
	End - DOY*	319	
Average Wind Speed (mph)*		7.50	(1)
Average RH*	1st Quarter	58.5%	(1)
	2nd Quarter	30.7%	
	3rd Quarter	32.8%	
	4th Quarter	50.8%	
Precipitation*		Monthly Variation	(2)
Temperature (min and max)*		Monthly Variation	(2)
Solar Radiation*		Based on Latitude of 37.52 Degrees	(2)

* Parameter Varied
(1) Abraham and Waugh (1995)
(2) Owenby and Ezell (1992)

Uncertainty Distributions for Layer 1

The RETC Program (van Genuchten, et al., 1991) has been used to fit the initial drainage curve data for the Monticello soils (Daniel B. Stephens & Associates, 1993). The resulting fitting parameters, as well as the porosity, field capacity, and wilting point have been derived from these fits. Initially, the Brooks and Corey option was selected in RETC because Brooks and Corey is used in HELP, but the fits did not make sense. The van Genuchten/Mualem option (m=1-1/n) was selected next, and the fits were much better. The saturation as a function of head for van Genuchten is

$$S_e = \left(1+(\alpha h)^n\right)^{-m}$$

where m = 1 – 1/n for the Mualem option, and

$$S_e = \frac{\theta - \theta_r}{\theta_s - \theta_r}$$

where α, n, θ_s and θ_r were fit by the program. The results are tabulated below as well as the field capacity (θ_{FC}) (h=0.33 bars = 330 cm) and wilting point (θ_{WP}) (h=15 bars = 15,000 cm) derived from the fit. The porosity was calculated from the curve fit and is different from the porosity listed in the report.

Table A-3. Constitutive parameters for soil samples of layer 1.

Sample Number	Porosity $\phi=\theta_s$	α (cm^{-1})	n	θ_r	θ_{FC}	θ_{WP}	R^2
358-128	0.474	0.0412	1.142	0.	0.326	0.191	0.972
358-144	0.427	0.0032	1.183	0.	0.381	0.209	0.979
358-172	0.373	0.00026	1.249	0.	0.370	0.257	0.993
351-128	0.468	0.0616	1.146	0.	0.301	0.173	0.972
351-144	0.398	0.0033	1.188	0.	0.354	0.192	0.968
351-172	0.356	0.00027	1.267	0.	0.353	0.237	0.996
354-128	0.462	0.0410	1.295	0.0153	0.221	0.082	0.998
354-144	0.466	0.0144	1.337	0.0236	0.278	0.096	0.991
354-188	0.332	0.0048	1.217	0.	0.278	0.132	0.964
361-128	0.391	0.0606	1.155	0.	0.245	0.136	0.985
361-144	0.408	0.0341	1.156	0.	0.277	0.154	0.980
361-177	0.330	0.00072	1.230	0.	0.321	0.189	0.984

The R^2 values are generally good for all the fits. However, because the data are limited (8 points per curve for pressure heads ranging from 0 to over 100,000 cm), the fidelity of the curve fits may be low. The fits show a wide range of values, especially for the α parameter, which ranges over two orders of magnitude. The porosity values from the curve fits are generally much lower than the porosity values listed in the report. The values from the curve fit tend towards the measured moisture content at zero head. Even with the wide variation in the α parameter, the calculated values of the field capacity (θ_{FC}) and wilting point (θ_{WP}) are reasonably consistent except for a couple of values.

A statistical analysis of the parameters in Table A-3 was performed to estimate the uncertainty distributions and potential correlations among saturated hydraulic conductivity, field capacity, and wilting point. The probability plot of log-transformed K_{sat} indicates an approximately log-normal distribution for this parameter, with the exception of one outlier sample, as shown in Figure A-1 below. The mean value of log K_{sat} is –3.52 with a standard deviation of approximately 0.95.

The linear correlation between log K_{sat} and field capacity gives a negative correlation with an R-squared value of 0.44. The linear correlation between field capacity and wilting point yields a positive correlation with an R-squared value of 0.78. Both field capacity and wilting point appear to be approximately uniformly distributed.

Results indicate that K_{sat} should be sampled from a log-normal distribution with a log-transformed mean of –3.52 and standard deviation of 0.95. Field capacity should be sampled from a uniform distribution with a lower bound of 0.22 and upper bound of 0.38. Wilting point should be sampled from a uniform distribution with a lower bound of 0.08 and an upper bound of 0.21. A correlation coefficient of negative 0.44 should be specified for log K_{sat} and field capacity. A correlation coefficient of 0.78 should be specified for field capacity and wilting point.

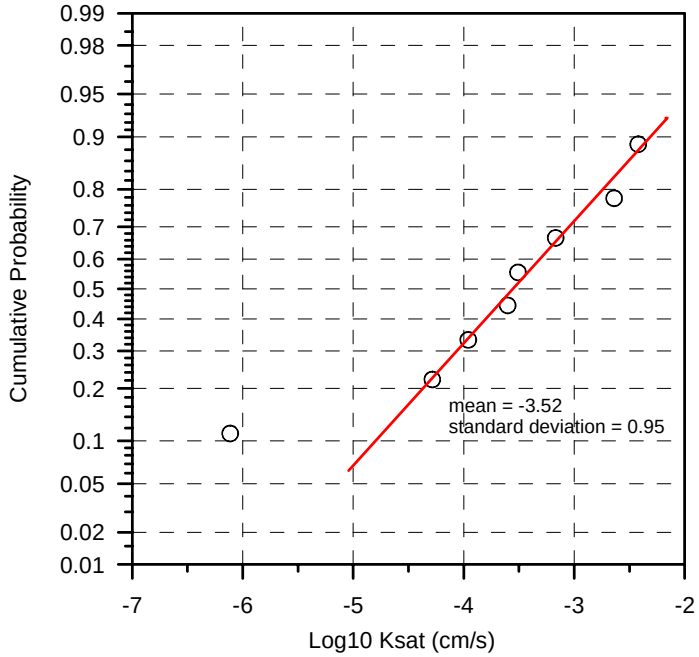

Figure A-1. Cumulative probability of log-transformed hydraulic conductivity for soil samples of layer 1.

Uncertainty Distributions for Layers 2 and 4

The section describes steps to develop stochastic parameter distributions for the saturated hydraulic conductivity (K_{sat}), wilting point (θ_{wp}), and field capacity (θ_{FC}). Uncertainty distributions for these parameters are developed for layers 2 (sand) and 4 (clay) of the HELP percolation model for the Monticello disposal site using data and joint probability distributions reported in Carsel and Parrish (1988).

1. Input statistics (mean and standard deviation) for normal (transformed) distributions of K_{sat}, α, and N for the sand and clay layers in Carsel and Parrish (1988, Table 6) into LHS. Ensure physical limits of parameters by transforming lower and upper bounds (A and B) for lognormal and hyperbolic arcsine transforms (do not need limits on log ratio transform). The only parameters that need to have physical limits applied are the N-parameters for both sand and clay layers (lognormal transforms).

2. Input correlation coefficients into LHS for K_{sat}, α, and N using the lower triangular portion of the matrices shown in Table 7 of Carsel and Parrish (1988). This lower triangular portion contains the "Pearson product-moment correlations," which is the same as the correlation coefficient, R, used in LHS.

3. After LHS has calculated the distribution of parameters, the parameters need to be post-processed and back-transformed into real space. In addition, the wilting point and field capacity need to be determined from the van Genuchten parameters (α and N). First, we

need to transform the LHS parameter so that its mean is the same as the mean used in the Monticello calculation. We convert the normalized LHS parameter, Y, to a standard normal deviate (say Z) and then convert the standard normal deviate to a value with a new mean assuming that the standard deviation in Carsel and Parrish (1988, Table 6) is the same as the Monticello data:

$y = Y + \mu 2 - \mu 1$

where y is the deviate in transformed space with the Monticello mean, Y is the transformed deviate sampled by LHS from the original distribution, $\mu 1$ is the mean from Carsel and Parrish (1988, Table 6), and $\mu 2$ is the Monticello mean. Note that $\mu 2$ is the mean in the transformed space. For a log-ratio transform, there is no analytical way to transform the mean value reported for Monticello to the log-ratio mean in transformed space (we would need the actual data; we only have site data for Layer 1 (soil), not layers 2 and 4). Therefore, we iterate on the transformed mean for the parameters that require a log-ratio transform in Carsel and Parrish (1988) (i.e., K_{sat} and α). This is done in a spreadsheet for all values in the distribution, and the transformed mean is varied until the desired mean is achieved for the distribution in real space. Because K_{sat} is generally lognormally distributed, we assumed that the point values for K_{sat} used in the Monticello model were median values instead of mean values.

The van Genuchten N parameter for sand and clay uses a log-normal transformation in Carsel and Parrish (1988), so its transformed mean can be exactly specified from a mean value in real space (using the standard deviation from Carsel and Parrish). The mean N-parameter is obtained from the reported wilting point and field capacity in the Monticello calculation using the van Genuchten equation for soil moisture retention. The wilting point and field capacity values provide two equations for two unknowns, α and N. The wilting point and field capacity give the moisture content at capillary pressures of 0.33 and 15 bars, respectively. These equations can be solved implicitly, say, in Mathcad.

4. Backtransform the deviate from normal space (y) to real space (X) using the appropriate back-transformation (Eqs 15-17 in Carsel and Parrish, 1988).

5. Calculate wilting point by using a rearranged form of the van Genuchten equation. The following equation is taken from Equation 1 in Carsel and Parrish (1988), but the residual moisture content, θ_r, is replaced by the Equation (6) in the HELP Engineering Manual. In addition, the saturated moisture content is replaced by the porosity.

$$\theta_{wp} = \frac{a(\gamma - 1) + \phi}{\gamma + b(1 - \gamma)} \tag{A1}$$

$$\text{where} \quad \gamma = \left[1 + \left(\alpha h_{wp}\right)^N\right]^M \tag{A2}$$

$$\text{and} \quad a = 0.014,\ b = 0.25 \text{ if } \theta_{wp} \geq 0.04 \tag{A3}$$

$$a = 0,\ b = 0.6 \text{ if } \theta_{wp} < 0.04 \quad \text{(A4)}$$

where ϕ is the porosity of the material (not sampled), h_{wp} is the wilting point head (cm) associated with the wilting point pressure prescribed by HELP (p. 15 of the Engineering Manual) to be 15 bar (= 1.53×10^4 cm at 20ºC, and M = 1-1/N. Note that the resulting wilting point in (A1) must be compared to the conditions for the wilting point prescribed Equations (A3) and (A4). If the values are contradictory, then Equation (A1) must be solved again using the other values (either from Equation (A3) or Equation (A4)) for parameters *a* and *b*.

6. Once the wilting point is determined, the field capacity can be found using the Equation (A1) from Carsel and Parrish (1988):

$$\theta_{fc} = \theta_r + \frac{\phi - \theta_r}{\left[1 + \left(\alpha h_{fc}\right)^N\right]^M} \quad \text{(A5)}$$

$$\text{where } \theta_r = 0.014 + 0.25\theta_{wp} \text{ if } \theta_{wp} \geq 0.04 \quad \text{(A6)}$$

$$\theta_r = 0.6\theta_{wp} \text{ if } \theta_{wp} < 0.04 \quad \text{(A7)}$$

where h_{fc} is the field-capacity head (cm) associated with the field-capacity pressure prescribed by HELP (p. 15 of the Engineering Manual, Schroeder et al., 1994b) to be 0.33 bar (= 337 cm at 20ºC). This method assumes that the field capacity and the wilting point are perfectly correlated, and that they are calculated from the sampled van Genuchten parameters.

Distribution

1 Missy Klem
Department of Energy
P.O. Box 5400
Building 384-3
Albuquerque, NM 87185

1 Pam Saxman
Department of Energy
P.O. Box 5400
Building 384-3
Albuquerque, NM 87185

1 Michael Fayer
Battelle, Pacific Northwest National Laboratory
P.O. Box 999 / MS K9-33
Richland, WA 99352

1 Randal Taira
Battelle Seattle Research Center
4500 Sand Point Way NE
Suite 100
Seattle, WA 98105-3949

1 Gene Whelan
Battelle, Pacific Northwest National Laboratory
P.O. Box 999 / MS K9-36
Richland, WA 99352

1 Glendon Gee
Battelle, Pacific Northwest National Laboratory
P.O. Box 999 / MS K9-33
Richland, WA 99352

1 John Heiser
Brookhaven National Laboratory
P.O. Box 5000 , Building 830
Upton, NY 11973-5000

1 Jody Waugh
U.S. Department of Energy
Grand Junction Office
2597 B3/4 Road
Grand Junction, CO 81503

1 Mike Serrato
U.S. Department of Energy
Savannah River Operations Office
Road 1A, Building 773-42A
Aiken, SC 29801

1 Scott McMullin
U.S. Department of Energy
Savannah River Operations Office
Road 1A, Building 703-A
Aiken, SC 29801

1 Skip Chamberlain
Department of Energy, Headquarters
Germantown
19901 Germantown Road, Room 2218
Germantown, MD 20874-1290

1 James Wright
U.S. Department of Energy
Savannah River Operations Office
Road 1A, Building 703-A
Aiken, SC 29801

1	MS-0701	P. Davies, 6100
1	MS-0701	W. Cieslak, 6100
1	MS-0706	R. Finley, 6113
1	MS-0735	J. Cochran, 6115
10	MS-0735	C. Ho, 6115
1	MS-0735	E. Webb, 6115
1	MS-0750	M. Walck, 6116
1	MS-0751	L. Costin, 6117
1	MS-0750	H. Westrich, 6118
1	MS-0719	W. Cox, 6131
1	MS-0719	S. Dwyer, 6131
1	MS-0719	C. Heise, 6131
1	MS-0719	S. Howarth, 6131
1	MS-0719	E. Lindgren, 6131
1	MS-0719	S. Webb, 6131
1	MS-1087	F. Nimick, 6132
1	MS-1087	D. Stockham, 6133
1	MS-1088	D. Miller, 6134
1	MS-1089	D. Fate, 6135
1	MS-0771	M. Chu, 6800
1	MS-0771	S. Pickering, 6800
1	MS-0779	M. Marietta, 6800
1	MS-1395	K. Knowles, 6821
1	MS-0779	R. Anderson, 6849
1	MS-0779	J. Jones, 6849
1	MS-0778	P. Swift, 6851
1	MS-0778	M. Wilson, 6851
1	MS-0778	J. Gauthier, 6851
1	MS-0776	B. Arnold, 6852
1	MS-0776	H. Jow, 6852
1	MS-9018	Central Technical Files, 8945-1
2	MS-0899	Technical Library, 9616
1	MS-0612	Review & Approval Desk, 9612 For DOE/OSTI